

**Electronic Supplementary Information**

**Cyclometalated iridium(III) complexes induce mitochondria-derived  
paraptotic cell death and inhibit tumor growth *in vivo***

Liang He, Kang-Nan Wang, Yue Zheng, Jian-Jun Cao, Ming-Fang Zhang, Cai-Ping  
Tan, Liang-Nian Ji and Zong-Wan Mao\*

MOE Key Laboratory of Bioinorganic and Synthetic Chemistry, School of Chemistry, Sun Yat-sen  
University, Guangzhou 510275, P. R. China.

\*Corresponding author. E-mail address: cesmzw@mail.sysu.edu.cn (Z.W. Mao).

## Table of Contents

<b><u>Experimental section</u></b> .....	S4
Materials and measurements.....	S4
Synthesis and characterization.....	S5
Crystallographic structure determination.....	S8
Measurement of two-photon absorption (TPA) cross-section.....	S8
Cell lines and culture conditions.....	S9
Cytotoxicity .....	S9
Colocalization assay.....	S9
Cellular uptake and distribution (ICP-MS).....	S10
Lipophilicity.....	S10
Cellular uptake mechanism studies.....	S10
Hoechst 33342 staining.....	S10
Annexin V staining assay.....	S11
Western blotting.....	S11
Caspase-3/7 activity assay.....	S11
Monodansylcadaverine (MDC) staining assay.....	S11
Transmission electron microscopy (TEM).....	S11
Inhibition of 20S proteasomal activity in cultured cells.....	S12
Measurement of mitochondrial membrane potential.....	S12
Intracellular ATP detection.....	S12
Mitochondrial bioenergetics analysis.....	S12
ROS detection.....	S13
<i>In vivo</i> antitumor evaluation of complex <b>IrM2</b> .....	S13
Histological analysis (H&E staining).....	S14

Immunohistochemical Staining.....	S14
Statistical analysis.....	S14
<b><u>Supporting figures and tables</u></b> .....	S15
Fig. S1-S6 <sup>1</sup> H NMR spectra of <b>L1</b> , <b>L2</b> and <b>IrM1–IrM4</b> .....	S15
Fig. S7 & S8 UV-Vis spectra and emission spectra of <b>IrM1–IrM4</b> .....	S18
Fig. S9 Two-photon absorption cross-sections of <b>IrM1–IrM4</b> .....	S19
Fig. S10-S12 Colocalization assays with MTG, LTG or ERG.....	S19
Fig. S13 Cellular uptake mechanism of <b>IrM2</b> .....	S21
Fig. S14 Images of Hoechst stained HeLa, HepG2 and MCF-7 cells.....	S22
Fig. S15 Representative confocal images of annexin V labeled A549 cells.....	S22
Fig. S16 Detection of caspase-3/7 activity.....	S23
Fig. S17 Representative confocal images of MDC stained A549 cells.....	S24
Fig. S18 Effects of various autophagy inhibitors on cell viability.....	S25
Fig. S19 Detection of cellular proteasomal activity.....	S26
Fig. S20 Effects of various inhibitors on cell viability.....	S27
Fig. S21 Effects of <b>IrM2</b> on MMP analyzed by confocal microscopy.....	S27
Fig. S22 Effects of various ROS inhibitors on cell viability.....	S28
Fig. S23 Superoxide detected by MitoSOX-Red.....	S28
Table S1&S2 Crystallographic data.....	S29
Table S3 Photophysical data.....	S31
Table S4 Lipophilicity and cellular uptake of <b>IrM1–IrM4</b> .....	S31
<b><u>Supporting references</u></b> .....	S32

## Experimental section

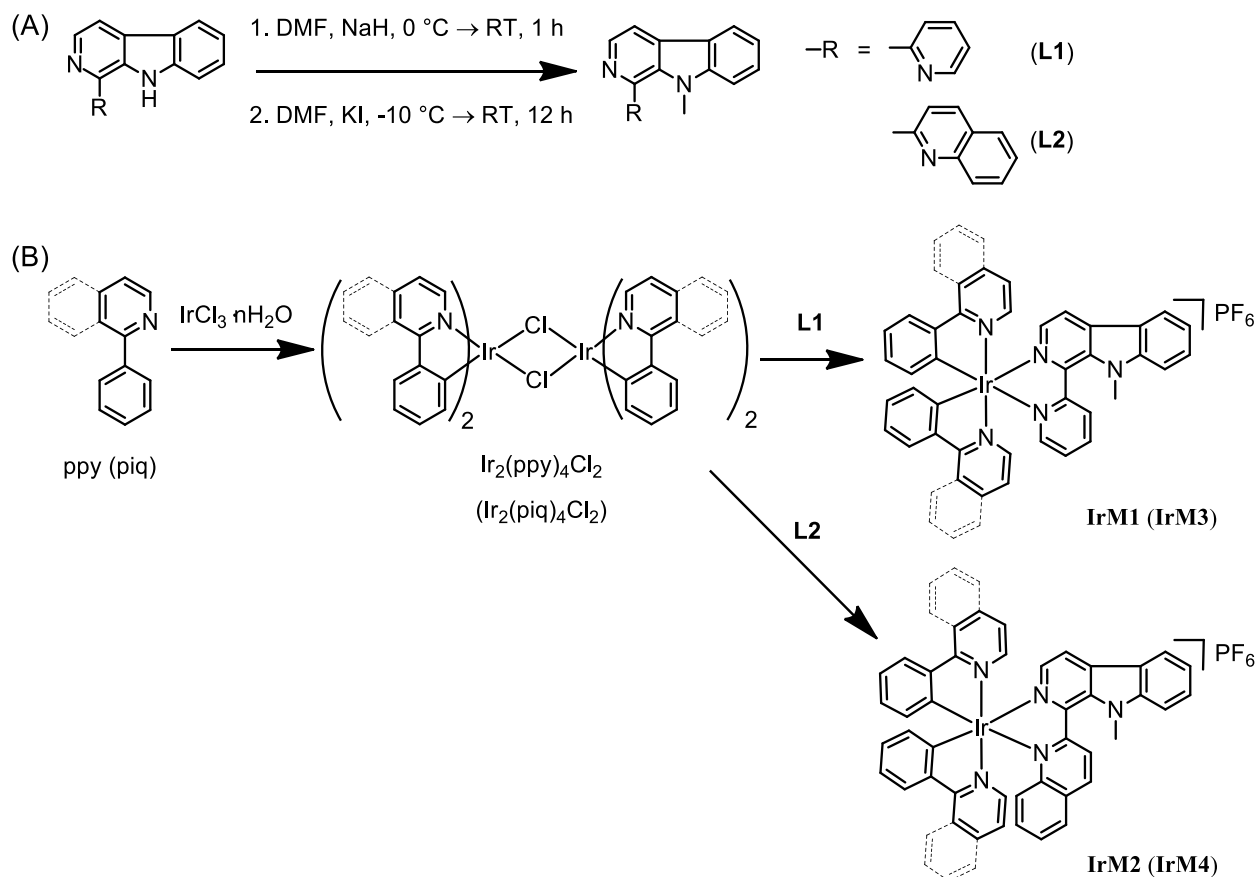
### Materials and measurements

Sodium hydride (Alfa Aesar, USA), potassium iodide (Alfa Aesar, USA), iridium chloride hydrate (Alfa Aesar, USA), 2-phenylpyridine (ppy, Sigma Aldrich, USA), 1-phenylisoquinoline (piq, Sigma Aldrich, USA), cisplatin (Sigma Aldrich, USA), dimethyl Sulphoxide (DMSO, Sigma Aldrich, USA), 3-(4,5-dimethylthiazol-2-yl)-2,5-diphenyltetrazolium bromide (MTT, Sigma Aldrich, USA), phosphate buffered saline (PBS, Sigma Aldrich, USA), MitoTracker Green FM (MTG, Life Technologies, USA), LysoTracker Green DND-26 (LTG, Life Technologies, USA), ER-Tracker Green (ERG, Life Technologies, USA), carbonyl cyanide *m*-chlorophenyl hydrazone (CCCP, Sigma Aldrich, USA), chloroquine (CQ, Sigma Aldrich, USA), Hoechst 33342 (Sigma Aldrich, USA), z-VAD-fmk (Sigma Aldrich, USA), monodansylcadaverine (MDC, Sigma Aldrich, USA), tamoxifen (Cayman Chemical, USA), 3-methyladenine (3-MA, Sigma Aldrich, USA), wortmannin (Cayman Chemical, USA), bafilomycin A1 (Santa Cruz Biotechnology, USA), 4-phenylbutyric acid (Sigma Aldrich, USA), cycloheximide (CHX, Sigma Aldrich, USA), necrostatin-1 (Santa Cruz Biotechnology, USA), rhodamine 123 (Sigma Aldrich, USA), 2',7'-dichlorofluorescein diacetate (H<sub>2</sub>DCF-DA, Sigma Aldrich, USA), *N*-acetyl-*L*-cysteine (NAC, Sigma Aldrich, USA), MnTBAP (Santa Cruz Biotechnology, USA), catalase (Sigma Aldrich, USA), mannitol (J&K Scientific Ltd, China), KI (J&K Scientific Ltd, China) and sodium azide (Sigma Aldrich, USA) were used as received. Annexin V-FITC apoptosis detection kit was purchased from Sigma Aldrich (USA). Proteasome 20S Activity Assay Kit was purchased from Abcam (UK). Caspase-3/7 activity kit was purchased from Promega (USA). All antibodies were purchased from Cell Signaling Technology (USA) and used as recommended by the manufacturer.

All the compounds tested were first dissolved in DMSO before the experiments, and the final concentration of DMSO was kept at 1% (v/v). NMR spectra were recorded on a Bruker Avance 400 spectrometer (Germany). ESI-MS spectra were recorded on a Thermo Finnigan LCQ DECA XP spectrometer (USA). The quoted *m/z* values represented the major peaks in the isotopic distribution. Microanalysis (C, H, N and S) was carried out using an Elemental Vario EL CHNS analyzer (Germany). UV/Vis spectra were recorded on a Varian Cary 300 spectrophotometer (USA).

Steady-state emission spectra and lifetime measurements were conducted on a combined fluorescence lifetime and steady state spectrometer FLS 920 (UK). Cell imaging experiments were carried out on a confocal microscope (LSM 800 with Airyscan, ZEISS, Germany). Flow cytometric analysis was done using a BD FACS Calibur™ flow cytometer (Becton Dickinson, USA).

### Synthesis and characterization



**Scheme S1.** Synthetic procedures of (A) indolo-*N*-methylated  $\beta$ -carboline derivatives **L1** and **L2**, and (B) Ir(III) complexes **IrM1** and **IrM2**.

1-(2-pyridyl)- $\beta$ -carboline and 1-(2-quinolonyl)- $\beta$ -carboline were synthesized as previously reported.<sup>1</sup> The dimeric Ir(III) precursors  $[\text{Ir}_2(\text{ppy})_4\text{Cl}_2]$  and  $[\text{Ir}_2(\text{piq})_4\text{Cl}_2]$  were prepared according to a similar procedure described in the literature.<sup>2</sup>

**9-methyl-1-(2-pyridyl)- $\beta$ -carboline (L1):** A mixture of 1-(2-pyridyl)- $\beta$ -carboline (245 mg, 1.0 mmol) and anhydrous DMF (6 mL) was stirred at 0 °C, and then 95% NaH (38 mg, 1.5 mmol) was

added. The mixture was allowed to reach room temperature and stirred for 1 h. The mixture was cooled to  $-10\text{ }^{\circ}\text{C}$  and continued to stir, and then iodomethane (166 mg, 1.0 mmol) dissolved in anhydrous DMF (5 mL) was added dropwise and stirred for 15 min. Thereafter, the mixture was allowed to reach room temperature and stirred for 12 h. The solution was poured into water (30 mL) and the resulting solid product was collected. The product obtained was purified by silica column chromatography with dichloromethane and methanol as the eluent. Ligand **L1** was obtained as a light yellow powder. Yield: 0.216 g (83%).  $^1\text{H NMR}$  (500 MHz,  $d_6$ -DMSO):  $\delta$  = 8.73 (d,  $J$  = 4.7 Hz, 1H, H<sub>10</sub>), 8.45 (d,  $J$  = 5.1 Hz, 1H, H<sub>7</sub>), 8.32 (d,  $J$  = 7.8 Hz, 1H, H<sub>1</sub>), 8.24 (d,  $J$  = 5.1 Hz, 1H, H<sub>3</sub>), 8.01 (td,  $J$  = 7.7, 1.6 Hz, 1H, H<sub>2</sub>), 7.95 (d,  $J$  = 7.7 Hz, 1H, H<sub>9</sub>), 7.68–7.60 (m, 2H, H<sub>4</sub> and H<sub>5</sub>), 7.53–7.49 (m, 1H, H<sub>6</sub>), 7.31 (t,  $J$  = 7.2 Hz, 1H, H<sub>8</sub>), 3.51 (s, 3H, H<sub>11</sub>). ESI-MS (CH<sub>3</sub>OH):  $m/z$  calcd for  $[\text{M}+\text{H}]^+$ , 259.3; found: 259.1. Elemental analysis calcd (%) for C<sub>17</sub>H<sub>13</sub>N<sub>3</sub>: C, 78.74; H, 5.05; N, 16.20; found: C, 78.69; H, 5.11; N, 16.16.

**9-methyl-1-(2-quinolinyl)- $\beta$ -carboline (L2):** Ligand **L2** was synthesized by a similar method described for **L1**. Ligand **L2** was obtained as a light yellow powder. Yield: 0.235 g (76%).  $^1\text{H NMR}$  (400 MHz,  $d_6$ -DMSO):  $\delta$  = 8.57 (dd,  $J$  = 14.8, 6.6 Hz, 2H, H<sub>1</sub> and H<sub>10</sub>), 8.36 (dd,  $J$  = 20.4, 6.1 Hz, 2H, H<sub>3</sub> and H<sub>9</sub>), 8.25–8.09 (m, 3H, H<sub>2</sub>, H<sub>7</sub> and H<sub>13</sub>), 7.86 (t,  $J$  = 7.4 Hz, 1H, H<sub>8</sub>), 7.69 (dt,  $J$  = 14.6, 7.4 Hz, 3H, H<sub>4</sub>, H<sub>5</sub> and H<sub>6</sub>), 7.36 (t,  $J$  = 7.1 Hz, 1H, H<sub>12</sub>), 3.64 (s, 3H, H<sub>11</sub>). ESI-MS (CH<sub>3</sub>OH):  $m/z$  calcd for  $[\text{M}+\text{H}]^+$ , 310.3; found: 310.1. Elemental analysis calcd (%) for C<sub>21</sub>H<sub>15</sub>N<sub>3</sub>: C, 81.53; H, 4.89; N, 13.58; found: C, 81.47; H, 4.94; N, 13.45.

**General procedures for the synthesis of complexes Ir1–Ir4:** A mixture of Ir<sub>2</sub>(C<sup>N</sup>)<sub>4</sub>Cl<sub>2</sub> (0.2 mmol, 1 equiv) and **L1/L2** (0.4 mmol, 2 equiv) in CH<sub>2</sub>Cl<sub>2</sub>/CH<sub>3</sub>OH (2:1, v/v) was heated to reflux under nitrogen for 4 h in the dark. The solution was cooled to room temperature and then a 6-fold excess of NH<sub>4</sub>PF<sub>6</sub> was added, and the mixture was stirred for another 1 h. The mixture was filtered and the filtrate was evaporated to dryness under reduced pressure. The solid obtained was dissolved in CH<sub>2</sub>Cl<sub>2</sub> and purified by column chromatography on silica gel eluted with CH<sub>2</sub>Cl<sub>2</sub>/acetone (10:1, v/v). The desired product was purified by recrystallization from CH<sub>2</sub>Cl<sub>2</sub>/diethyl ether.<sup>3</sup>

**[Ir(ppy)<sub>2</sub>(L1)](PF<sub>6</sub>) (IrM1).** Complex **IrM1** was obtained as orange crystals. Yield: 0.267 g (73%).

$^1\text{H}$  NMR (500 MHz,  $d_6$ -DMSO):  $\delta$  = 8.41–8.36 (m, 2H,  $\text{H}_1$  and  $\text{H}_{10}$ ), 8.31 (d,  $J$  = 7.9 Hz, 1H,  $\text{H}_7$ ), 8.25 (dd,  $J$  = 17.2, 8.3 Hz, 2H,  $\text{H}_{12}\times 2$ ), 8.18 (d,  $J$  = 8.2 Hz, 1H,  $\text{H}_3$ ), 8.05 (d,  $J$  = 5.7 Hz, 1H,  $\text{H}_2$ ), 7.92 (dd,  $J$  = 11.7, 6.1 Hz, 3H,  $\text{H}_9$  and  $\text{H}_{16}\times 2$ ), 7.85 (dd,  $J$  = 14.4, 6.2 Hz, 3H,  $\text{H}_6$  and  $\text{H}_{15}\times 2$ ), 7.79 (dd,  $J$  = 15.5, 6.9 Hz, 2H,  $\text{H}_{17}\times 2$ ), 7.72 (d,  $J$  = 5.5 Hz, 1H,  $\text{H}_4$ ), 7.64–7.59 (m, 1H,  $\text{H}_5$ ), 7.45 (t,  $J$  = 7.5 Hz, 1H,  $\text{H}_8$ ), 7.12–7.05 (m, 2H,  $\text{H}_{19}\times 2$ ), 7.01 (dd,  $J$  = 13.7, 6.9 Hz, 2H,  $\text{H}_{14}\times 2$ ), 6.90 (dd,  $J$  = 16.6, 8.0 Hz, 2H,  $\text{H}_{18}\times 2$ ), 6.25–6.19 (m, 2H,  $\text{H}_{13}\times 2$ ), 3.90 (s, 3H,  $\text{H}_{11}$ ). ESI-MS ( $\text{CH}_2\text{Cl}_2$ ):  $m/z$  calcd for  $[\text{M-PF}_6]^+$ , 759.9; found: 759.1. Elemental analysis calcd (%) for  $\text{C}_{39}\text{H}_{29}\text{N}_5\text{F}_6\text{PIr} \cdot 0.5\text{H}_2\text{O}$ : C, 51.26; H, 3.31; N, 7.66; found: C, 51.18; H, 3.37; N, 7.59.

**[Ir(ppy) $_2$ (L2)](PF $_6$ ) (IrM2).** Complex **IrM2** was obtained as red crystals. Yield: 0.306 g (80%).  $^1\text{H}$  NMR (500 MHz,  $d_6$ -DMSO):  $\delta$  = 8.78 (d,  $J$  = 8.6 Hz, 1H,  $\text{H}_1$ ), 8.52 (d,  $J$  = 4.6 Hz, 1H,  $\text{H}_{10}$ ), 8.39 (dd,  $J$  = 7.1, 4.5 Hz, 2H,  $\text{H}_{14}\times 2$ ), 8.32 (d,  $J$  = 7.8 Hz, 1H,  $\text{H}_3$ ), 8.22 (d,  $J$  = 8.2 Hz, 1H,  $\text{H}_9$ ), 8.08 (d,  $J$  = 8.0 Hz, 1H,  $\text{H}_2$ ), 8.04 (d,  $J$  = 8.2 Hz, 1H,  $\text{H}_7$ ), 7.92–7.84 (m, 4H,  $\text{H}_{17}\times 2$  and  $\text{H}_{18}\times 2$ ), 7.80 (t,  $J$  = 7.2 Hz, 2H,  $\text{H}_{19}\times 2$ ), 7.74 (t,  $J$  = 7.9 Hz, 1H,  $\text{H}_{13}$ ), 7.69 (d,  $J$  = 5.8 Hz, 1H,  $\text{H}_8$ ), 7.65 (d,  $J$  = 5.6 Hz, 1H,  $\text{H}_4$ ), 7.56 (t,  $J$  = 7.5 Hz, 1H,  $\text{H}_5$ ), 7.46 (t,  $J$  = 7.4 Hz, 1H,  $\text{H}_6$ ), 7.16 (t,  $J$  = 7.8 Hz, 1H,  $\text{H}_{21}$ ), 7.07 (t,  $J$  = 6.6 Hz, 1H,  $\text{H}_{21}$ ), 6.99 (ddd,  $J$  = 18.5, 14.9, 7.3 Hz, 3H,  $\text{H}_{12}$  and  $\text{H}_{16}\times 2$ ), 6.91 (dt,  $J$  = 12.4, 6.0 Hz, 2H,  $\text{H}_{20}\times 2$ ), 6.31 (d,  $J$  = 7.2 Hz, 1H,  $\text{H}_{15}$ ), 6.05 (d,  $J$  = 7.6 Hz, 1H,  $\text{H}_{15}$ ), 3.88 (s, 3H,  $\text{H}_{11}$ ). ESI-MS ( $\text{CH}_2\text{Cl}_2$ ):  $m/z$  calcd for  $[\text{M-PF}_6]^+$ , 810.0; found: 810.1. Elemental analysis calcd (%) for  $\text{C}_{43}\text{H}_{31}\text{N}_5\text{F}_6\text{PIr}$ : C, 54.08; H, 3.27; N, 7.33; found: C, 54.11; H, 3.34; N, 7.31.

**[Ir(piq) $_2$ (L1)](PF $_6$ ) (IrM3).** Complex **IrM3** was obtained as red crystals. Yield: 0.274 g (67%).  $^1\text{H}$  NMR (500 MHz,  $d_6$ -DMSO):  $\delta$  = 9.06–9.01 (m, 1H,  $\text{H}_{10}$ ), 8.95 (dd,  $J$  = 6.3, 3.5 Hz, 1H,  $\text{H}_1$ ), 8.41 (t,  $J$  = 7.2 Hz, 2H,  $\text{H}_{18}\times 2$ ), 8.35 (d,  $J$  = 5.6 Hz, 1H,  $\text{H}_7$ ), 8.31 (d,  $J$  = 8.1 Hz, 1H,  $\text{H}_3$ ), 8.25 (ddd,  $J$  = 10.6, 9.1, 4.6 Hz, 2H,  $\text{H}_{12}\times 2$ ), 8.05 (ddd,  $J$  = 9.7, 7.9, 4.8 Hz, 3H,  $\text{H}_2$  and  $\text{H}_{17}\times 2$ ), 7.89 (dd,  $J$  = 5.9, 3.7 Hz, 2H,  $\text{H}_{14}\times 2$ ), 7.86–7.81 (m, 3H,  $\text{H}_9$  and  $\text{H}_{19}\times 2$ ), 7.78 (dd,  $J$  = 16.4, 6.9 Hz, 2H,  $\text{H}_{21}\times 2$ ), 7.72 (d,  $J$  = 6.5 Hz, 1H,  $\text{H}_6$ ), 7.61–7.54 (m, 3H,  $\text{H}_4$  and  $\text{H}_{15}\times 2$ ), 7.53 (d,  $J$  = 6.5 Hz, 1H,  $\text{H}_5$ ), 7.43 (t,  $J$  = 7.5 Hz, 1H,  $\text{H}_8$ ), 7.12 (q,  $J$  = 7.5 Hz, 2H,  $\text{H}_{20}\times 2$ ), 6.96–6.87 (m, 2H,  $\text{H}_{16}\times 2$ ), 6.23 (t,  $J$  = 8.5 Hz, 2H,  $\text{H}_{13}\times 2$ ), 3.94 (s, 3H,  $\text{H}_{11}\times 3$ ). ESI-MS ( $\text{CH}_2\text{Cl}_2$ ):  $m/z$  calcd for  $[\text{M-PF}_6]^+$ , 860.0; found: 860.2. Elemental analysis calcd (%) for  $\text{C}_{47}\text{H}_{33}\text{N}_5\text{F}_6\text{PIr} \cdot \text{H}_2\text{O}$ : C, 55.18; H, 3.45; N, 6.85; found: C, 55.10; H, 3.43; N, 6.81.

**[Ir(piq)<sub>2</sub>(L2)](PF<sub>6</sub>) (IrM4)**. Complex **IrM4** was obtained as red crystals. Yield: 0.305 g (71%). <sup>1</sup>H NMR (500 MHz, *d*<sub>6</sub>-DMSO):  $\delta$  = 9.01 (d, *J* = 9.1 Hz, 1H, H<sub>1</sub>), 8.78 (dd, *J* = 19.1, 8.3 Hz, 2H, H<sub>20</sub>×2), 8.59 (d, *J* = 6.3 Hz, 1H, H<sub>10</sub>), 8.41 (d, *J* = 8.7 Hz, 1H, H<sub>9</sub>), 8.38–8.33 (m, 2H, H<sub>14</sub>×2), 8.31–8.24 (m, 2H, H<sub>19</sub>×2), 8.07–8.03 (m, 1H, H<sub>3</sub>), 8.00 (d, *J* = 8.1 Hz, 1H, H<sub>13</sub>), 7.96–7.92 (m, 1H, H<sub>7</sub>), 7.85 (dd, *J* = 8.6, 5.2 Hz, 3H, H<sub>2</sub> and H<sub>16</sub>×2), 7.81–7.74 (m, 4H, H<sub>21</sub>×2 and H<sub>23</sub>×2), 7.62 (d, *J* = 6.5 Hz, 1H, H<sub>8</sub>), 7.54 (d, *J* = 6.5 Hz, 1H, H<sub>12</sub>), 7.52–7.40 (m, 3H, H<sub>6</sub> and H<sub>17</sub>×2), 7.34 (d, *J* = 6.5 Hz, 1H, H<sub>4</sub>), 7.13 (dt, *J* = 16.3, 8.0 Hz, 3H, H<sub>5</sub> and H<sub>22</sub>×2), 6.95 (dd, *J* = 15.9, 7.9 Hz, 2H, H<sub>18</sub>×2), 6.29 (d, *J* = 7.6 Hz, 1H, H<sub>15</sub>), 6.15 (d, *J* = 7.6 Hz, 1H, H<sub>15</sub>), 3.92 (s, 3H, H<sub>11</sub>×3). ESI-MS (CH<sub>2</sub>Cl<sub>2</sub>): *m/z* calcd for [M-PF<sub>6</sub>]<sup>+</sup>, 910.1; found: 910.2. Elemental analysis calcd (%) for C<sub>51</sub>H<sub>35</sub>N<sub>5</sub>F<sub>6</sub>PIr H<sub>2</sub>O: C, 57.08; H, 3.48; N, 6.53; found: C, 57.05; H, 3.51; N, 6.50.

### **Crystallographic structure determination**<sup>3</sup>

Crystals of **IrM2**, **IrM3** and **IrM4** qualified for X-ray analysis were obtained by diffusion of diethyl ether to the dichloromethane solution. X-ray diffraction measurements were performed on a Bruker Smart 1000 CCD diffractometer with Cu or Mo K $\alpha$  radiation ( $\lambda$  = 1.54184 or 0.71073 Å) at 293 K or 298 K. The crystal structures of **IrM2**, **IrM3** and **IrM4** were solved by direct methods with program SHELXS and refined using the full-matrix least-squares program SHELXL.<sup>4</sup> The CCDC deposit numbers, crystallographic data, details of data collection and structure refinements are listed in Table S1. Selected bond distances and angles are listed in Table S2. The structural plots were drawn using the xp package in SHELXTL at a 50% thermal ellipsoids probability level.

### **Measurement of two-photon absorption (TPA) cross-section**

The TPA cross-sections were measured as previously reported.<sup>3</sup> Briefly, the two-photon excited phosphorescence spectra of complexes **IrM1–IrM4** at 710–870 nm in DMSO were acquired with a nanosecond pulsed laser (Opolette<sup>TM</sup> 355II; pulse width  $\leq$  100 fs; 80 MHz repetition rate; Spectra Physics Inc., USA) by using rhodamine B as the reference.<sup>5</sup> The two-photon excited phosphorescence intensities of the reference and samples emitted at the same excitation wavelength were determined. The TPA cross sections were calculated according to the following equation.<sup>6</sup>



$$\delta_s = \delta_r \frac{\Phi_r c_r I_s n_s}{\Phi_s c_s I_r n_r}$$

Where  $I$  is the integrated fluorescence intensity,  $c$  is the concentration,  $n$  is the refractive index,  $\Phi$  is the quantum yield, subscript 'r' stands for reference samples, and 's' stands for the samples.

### **Cell lines and culture conditions**

A549, A549R, HeLa, MCF-7, HepG2 and LO2 cells were obtained from Experimental Animal Center of Sun Yat-sen University (Guangzhou, China). The cells were maintained in RPMI 1640 (Roswell Park Memorial Institute 1640, Gibco BRL) or DMEM (Dulbecco's modified Eagle's medium, Gibco BRL) medium, which contained 10% FBS (fetal bovine serum, Gibco BRL), 100  $\mu\text{g}/\text{mL}$  streptomycin (Gibco BRL), and 100 U/mL penicillin (Gibco BRL). The cells were cultured in a humidified incubator, which provided an atmosphere of 5%  $\text{CO}_2$  and 95% air at a constant temperature of 37  $^\circ\text{C}$ . In each experiment, cells treated with vehicle control (1% DMSO) were kept as the reference group.

### **Cytotoxicity**

The cytotoxicity of the tested compounds towards the indicated cell lines was determined by an MTT assay. The cells were cultured in 96-well plates and grown to confluence. The compounds tested were first dissolved in DMSO and immediately diluted with fresh media. The final concentration of DMSO was kept at 1% (v/v). The cells were incubated with a series of concentrations of the tested compounds for 44 h. MTT solution (20  $\mu\text{L}$ ) was then added to each well, and the cells were incubated for an additional 4 h. The media was carefully removed, and DMSO was added (150  $\mu\text{L}$  per well) and incubated for 10 min with shaking. The absorbance at 590 nm was measured using a microplate reader (Infinite M200 Pro, Tecan, Männedorf, Switzerland).

### **Colocalization assay**

The cells were first stained with MTG (150 nM), LTG (150 nM) or ERG (5  $\mu\text{M}$ ) for 30 min at 37  $^\circ\text{C}$ , and then further incubated with complexes **IrM1** (1  $\mu\text{M}$ ), **IrM2** (1  $\mu\text{M}$ ), **IrM3** (4  $\mu\text{M}$ ) or **IrM4** (4  $\mu\text{M}$ ) for 10 min. The cells were washed three times with PBS and visualized by confocal microscopy (LSM 710, Carl Zeiss, Göttingen, Germany) with a 63 $\times$  oil-immersion objective lens immediately.

(Note that higher Ir(III) concentrations or longer treatment time could cause a significant impact on mitochondrial integrity, leading to the failure of mitochondrial staining of MTG!) The wavelengths for one- and two-photon excitation of Ir(III) complexes are 488 nm and 810 nm, respectively. The excitation wavelength of MTG, LTG and ERG is 488 nm. Emission was collected at 600–680 nm for Ir(III) complexes, 500–530 nm for MTG, LTG and ERG.

### **Cellular uptake and distribution (ICP-MS)**<sup>3</sup>

A549 cells were seeded in 10 cm tissue culture dishes and incubated for 24 h. The media was removed and replaced with fresh media containing the tested complexes (10  $\mu$ M). After 2 h incubation, the cells were washed three times with PBS, trypsinized, collected and subsequently divided into two equal parts. One part was for the extraction of mitochondrial portion and the other for the whole cell portion. Mitochondria were extracted by a Cell Mitochondria Isolation Kit (Beyotime, China). Finally, the part of whole cell portion and the part of mitochondrial extraction were digested with HNO<sub>3</sub> (65%, 0.2 mL) at room temperature for 24 h. The solution was then diluted to a final volume of 10 mL with Milli-Q water. The concentration of iridium was measured using the XSERIES 2 ICP-MS.

### **Lipophilicity**<sup>3</sup>

The lipophilicity of the Ir(III) complexes, which was presented as log  $P_{o/w}$  values, was determined according to a previously reported method.<sup>3</sup> Log  $P_{o/w}$  is defined as the logarithmic ratio of Ir(III) concentration in *n*-octanol to that in the aqueous phase.

### **Cellular uptake mechanism studies**

A549 cells were incubated with complex **IrM2** (2  $\mu$ M) at 4 or 37 °C for 10 min, or incubated with complex **IrM2** (2  $\mu$ M) at 37 °C for 2 h after pretreatment with CCCP (20  $\mu$ M) or CQ (50  $\mu$ M) for 1 h. The cells were washed twice with PBS and visualized by confocal microscopy (LSM 710, Carl Zeiss, Göttingen, Germany). Emission was collected at 600–680 nm upon excitation at 405 nm.

### **Hoechst 33342 staining**<sup>1</sup>

A549 cells were treated with the tested compounds for 24 h, and then washed twice with PBS and

fixed with 4% paraformaldehyde for 15 min at room temperature. The cells were washed twice with PBS, and then Hoechst 33342 (5  $\mu\text{g}/\text{mL}$ ) in PBS was added to the medium by gently shaking in the dark for 10 min. The cells were washed twice with PBS and visualized by confocal microscopy (LSM 710, Carl Zeiss, Göttingen, Germany). Emission was collected at  $470 \pm 20$  nm upon excitation at 405 nm.

#### **Annexin V staining assay**

The assay was performed according to the method previously reported.<sup>7</sup> The assay was performed according to the manufacturer's (Sigma Aldrich, USA) protocol. Emission was collected at  $530 \pm 20$  nm upon excitation at 488 nm.

#### **Western blotting**

The assays were performed according to similar procedures previously reported.<sup>7</sup>

#### **Caspase-3/7 activity assay**

The assay was performed according to the method previously reported.<sup>7</sup> Caspase-3/7 activity was measured using Caspase-Glo Assay kit (Promega, USA) according to the manufacturer's instructions.

#### **Monodansylcadaverine (MDC) staining assay**

A549 cells seeded in 35 mm tissue culture dishes (Corning, USA) were exposed to the tested compounds at the indicated concentrations for 12 h. The cells were washed twice with PBS and then stained with MDC (50  $\mu\text{M}$  in PBS) at 37 °C for 10 min in the dark. The cells were washed twice with PBS and visualized by confocal microscopy (LSM 710, Carl Zeiss, Göttingen, Germany). Emission was collected at  $520 \pm 10$  nm upon excitation at 405 nm.

#### **Transmission electron microscopy (TEM)<sup>7</sup>**

A549 cells were treated with 4  $\mu\text{M}$  IrM2 at 37 °C for different periods of time. The cells were collected and fixed overnight at 4 °C in phosphate buffer (pH 7.4) containing 2.5% glutaraldehyde. The cells were then treated with osmium tetroxide, stained with uranyl acetate and lead citrate, and visualized under a transmission electron microscope (JEM 100 CX, JEOL, Tokyo, Japan). Images

were photographed using the Eversmart Jazz program (Scitex).

### **Inhibition of 20S proteasomal activity in cultured cells**

The assay was performed using Proteasome 20S Activity Assay Kit (Abcam, UK) according to the manufacturer's instructions. A549 cells cultured in 96-well plates were treated with different concentrations of **IrM2** or 5  $\mu$ M MG132 for 6 h. After an additional incubation with the specific fluorogenic peptide substrates for 2 h, the luminescence of hydrolyzed production was measured using a microplate reader (Infinite M200 Pro, Tecan, Männedorf, Switzerland). The fluorogenic substrates LLVY-R110 (Abcam, UK), Bz-Val-Gly-Arg-AMC (Enzo Life Sciences, USA) and Suc-Leu-Leu-Val-Tyr-AMC (Enzo Life Sciences, USA) were used to determine the chymotrypsin-like, trypsin-like and PGPH-like activities of 20S proteasome, respectively.

### **Measurement of mitochondrial membrane potential**

**Flow cytometry.** A549 cells seeded into 6-well plates were treated with different concentrations of **IrM2** at 37  $^{\circ}$ C for 1 h. The cells were collected and incubated with 5  $\mu$ g/ml rhodamine 123 in serum-free RPMI 1640 at 37  $^{\circ}$ C for 30 min. The cells were washed twice with PBS, and the fluorescence intensity of the cells was measured by flow cytometry (FACSCalibur<sup>TM</sup>, Becton Dickinson, NJ, USA) with excitation at 488 nm and emission at 530 nm. Data were analysed by FlowJo software (Tree Star, OR, USA). Ten thousand events were acquired for each sample.

**Confocal microscopy.** A549 cells seeded in 35-mm tissue culture dishes (Corning, USA) were treated with different concentrations of **IrM2** at 37  $^{\circ}$ C for 1 h. The cells were washed twice with PBS and then incubated with 5  $\mu$ g/ml rhodamine 123 in serum-free RPMI 1640 at 37  $^{\circ}$ C for 30 min. The cells were washed twice with PBS and visualized immediately by confocal microscopy (LSM 710, Carl Zeiss, Göttingen, Germany). Emission was collected at 520  $\pm$  20 nm upon excitation at 488 nm.

### **Intracellular ATP detection**<sup>8</sup>

The assay was performed according to the method previously reported.<sup>8</sup> Cellular ATP level was measured using CellTiter-Glo<sup>®</sup> Luminescent Cell Viability Assay kit (G7570, Promega, USA) according to the manufacturer's instructions.

### **Mitochondrial bioenergetics analysis**<sup>8</sup>

The assay was performed according to the method previously reported.<sup>8</sup> The key parameters of mitochondrial function were assessed using the XF Cell Mito Stress Test Kit with the Seahorse XFe24 analyzer (Seahorse Bioscience, Billerica, USA) by directly measuring the oxygen consumption rate (OCR) according to the manufacturer's instructions.

### **ROS detection**

**Flow cytometry.** A549 cells seeded into 6-well plates were treated with different concentrations of **IrM2** at 37 °C for 1 h. The cells were collected and incubated with 10 μM H<sub>2</sub>DCF-DA for 20 min at 37 °C in the dark. The cells were washed twice with PBS, and the fluorescence intensity of DCF in A549 cells was measured by flow cytometry (FACSCalibur<sup>TM</sup>, Becton Dickinson, NJ, USA) with excitation at 488 nm and emission at 530 nm. Data were analysed by FlowJo software (Tree Star, OR, USA). Ten thousand events were acquired for each sample.

**Confocal microscopy.** A549 cells seeded in 35-mm tissue culture dishes (Corning, USA) were treated with **IrM2** (2 μM) at 37 °C for 1 h. The cells were washed twice with PBS and then incubated with 10 μM H<sub>2</sub>DCF-DA in serum-free RPMI 1640 for 20 min at 37 °C in the dark. The cells were washed twice with PBS and visualized immediately by confocal microscopy (LSM 710, Carl Zeiss, Göttingen, Germany). Emission was collected at 520 ± 20 nm upon excitation at 488 nm. To measure mitochondrial superoxide production, cells were loaded with 5 μM MitoSOX-Red for 10 min in the dark, washed with PBS, and visualized immediately by confocal microscopy. Emission was collected at 570–600 nm upon excitation at 514 nm.

### **In vivo antitumor evaluation of complex IrM2**

Female athymic nude mice aged 4–5 weeks were purchased from the Center of Experiment Animals at the Sun Yat-Sen University. All animal experiments were conducted under the guidelines approved by the Sun Yat-Sen University Animal Care and Use Committee. The nude mice were inoculated with A549 tumor cells by subcutaneous injection. When the average tumor size reached 100-120 mm<sup>3</sup>, the nude mice were randomly divided into three groups and treated with solvent control, complex **IrM2** (2.5 mg/kg), or cisplatin (2.5 mg/kg) (*n* = 4) every 3 days for 21 days by intraperitoneal injection. Complex **IrM2** was first dissolved in PET diluent (60% polyethylene

glycol 400, 30% ethanol, 10% Tween 80) and then diluted with PBS (PET:PBS = 1:9, v/v). The tumor sizes and body weights were measured every 3 days. The tumor volumes were calculated by the formula  $V = ab^2 \times 0.52$ , where  $a$  and  $b$  were the longest and shortest diameters of the xenografted tumor. After the experiment, the mice were sacrificed and tumors were separated. The tumor inhibition was calculated according to the following formula:

$$\text{Tumor growth inhibition rate (\%)} = \left(1 - \frac{V - V_0}{V' - V'_0}\right) \times 100\%$$

where  $V$  and  $V'$  are the tumor volumes of drug treatment group and solvent control group, respectively.  $V_0$  and  $V'_0$  are the initial tumor volumes of drug treatment group and solvent control group, respectively.

### **Histological analysis (H&E staining)**

All mice were sacrificed 21 days after the first drug treatment. Tumors were excised, fixed in formalin solution, and embedded in paraffin. Subsequently, tumor tissue was cut into sections and placed on the slides. The tissue sections were stained with hematoxylin-eosin (H&E) according to standard procedures, and examined under an inverted microscope at 200 $\times$  magnification.

### **Immunohistochemical Staining**

The formalin fixated and paraffin embedded tissue sections were deparaffinized, rehydrated, and washed with PBS. The tissue sections were blocked by 3% H<sub>2</sub>O<sub>2</sub> in methanol at room temperature for 30 min and subsequently washed with PBS three times. The tissue sections were then blocked by 5% BSA and incubated with primary antibody mouse MAb anti-PCNA (1:4000 dilution) at 4 °C overnight. After being washed with PBS for three times, the tissue sections were incubated with secondary antibody for 1 h at room temperature. Staining was developed in freshly prepared diaminobenzidine (DAB) solution, and slides were then counterstained with hematoxylin, dehydrated through graded ethanol, cleared with xylene, and cover-slipped. The cells were visualized with microscopy.

### **Statistical analysis**<sup>7</sup>

All biological experiments were performed at least twice with triplicates in each experiment. Representative results were depicted in this report and data were presented as means  $\pm$  standard deviations (SD).

## Supporting figures and tables

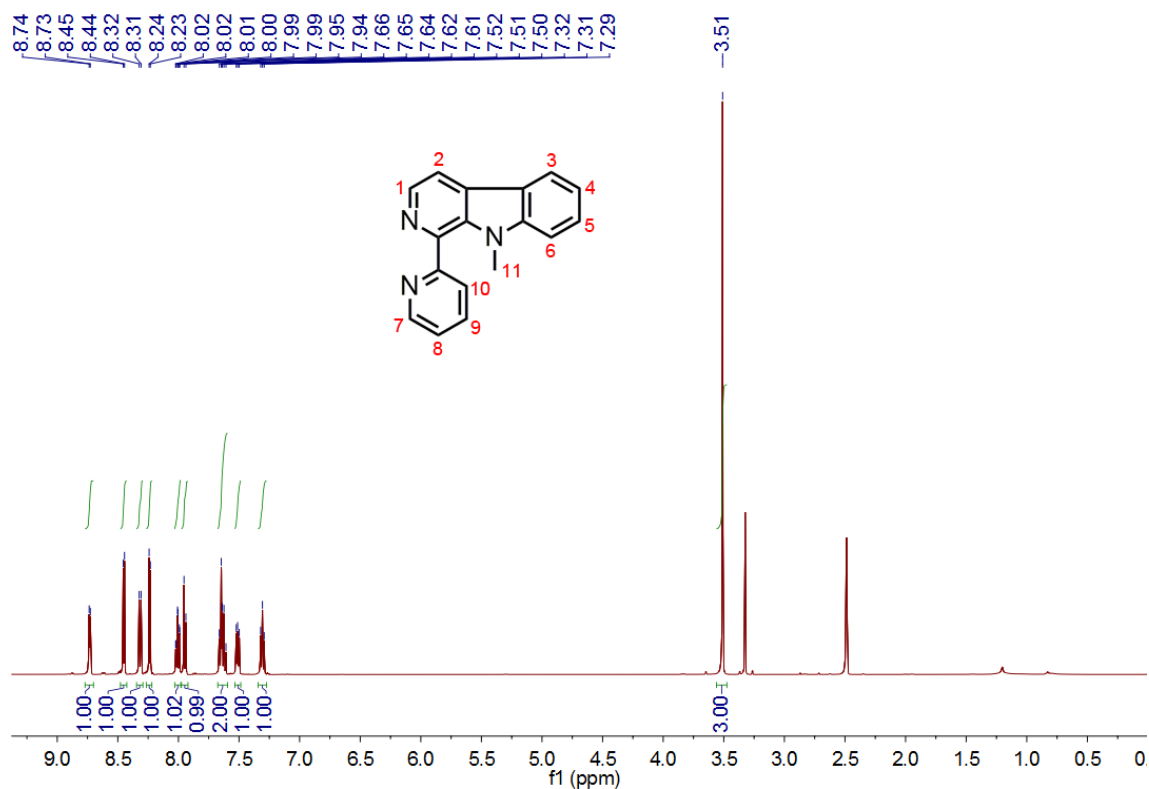


**Fig. S1**  $^1\text{H}$  NMR spectrum of **L1** in  $d_6$ -DMSO.

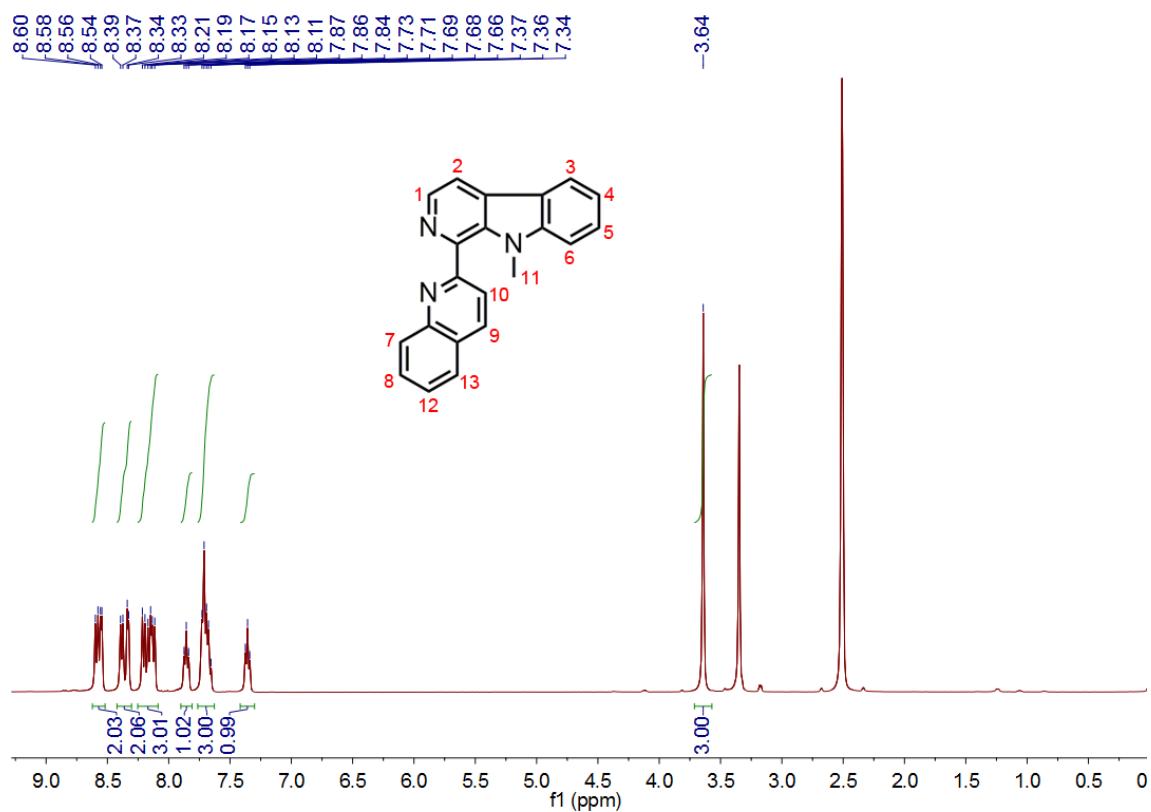


**Fig. S2**  $^1\text{H}$  NMR spectrum of **L2** in  $d_6$ -DMSO.

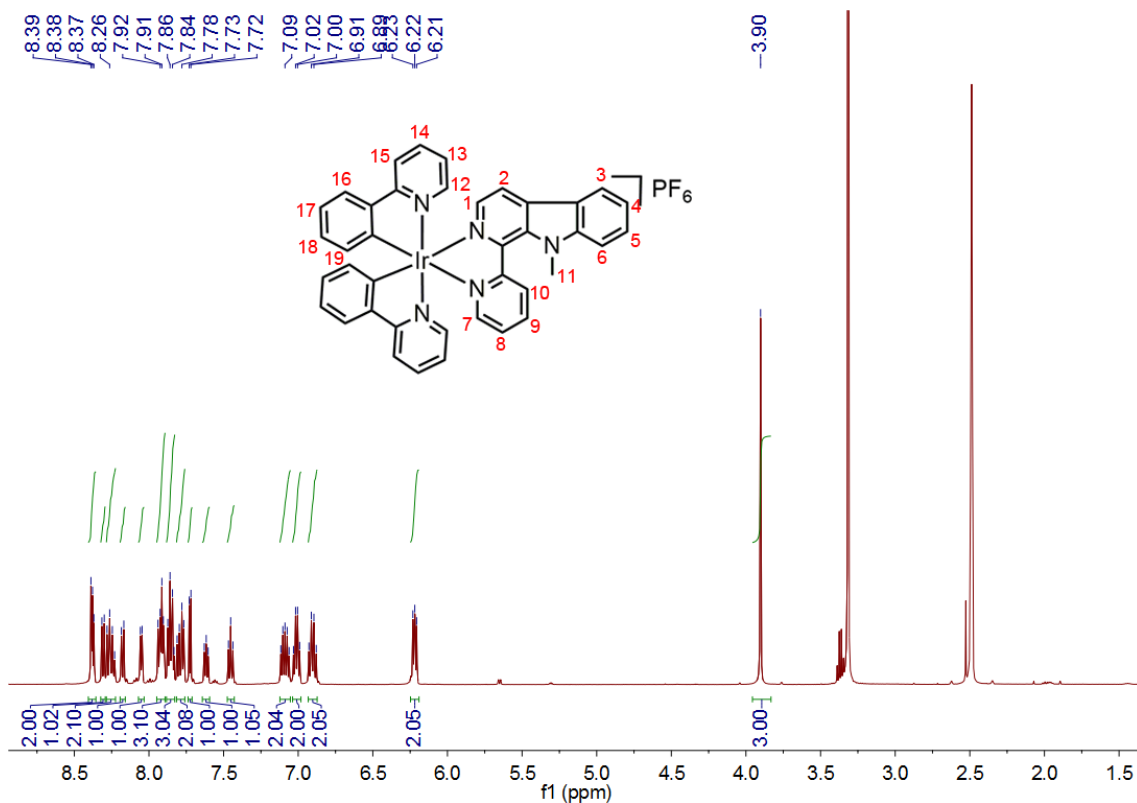


Fig. S3 <sup>1</sup>H NMR spectrum of IrM1 in d<sub>6</sub>-DMSO.

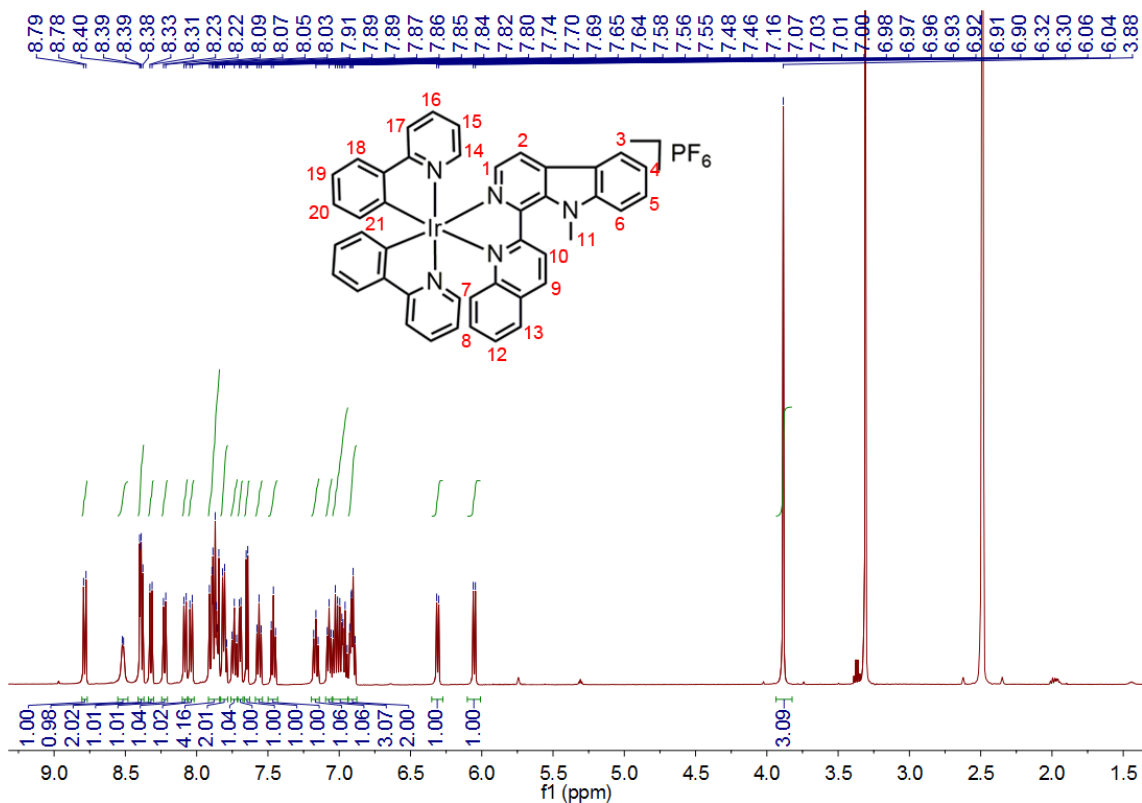


Fig. S4 <sup>1</sup>H NMR spectrum of IrM2 in d<sub>6</sub>-DMSO.



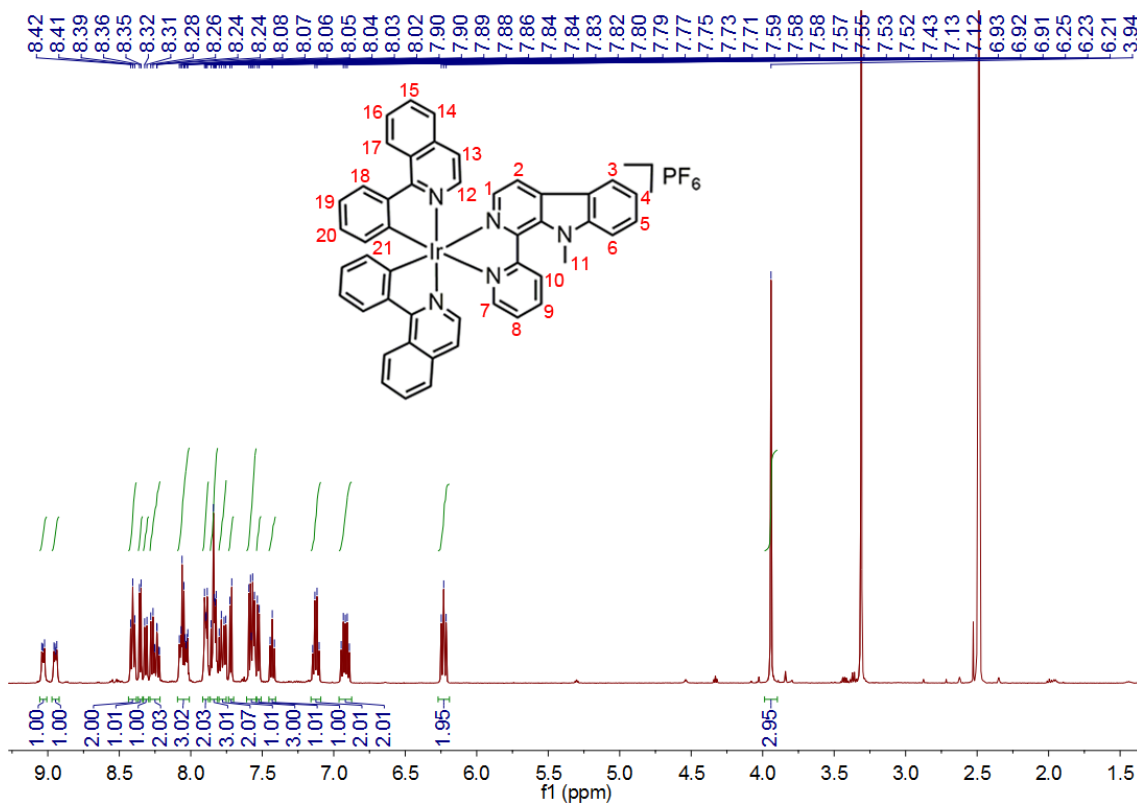


Fig. S5 <sup>1</sup>H NMR spectrum of IrM3 in d<sub>6</sub>-DMSO.

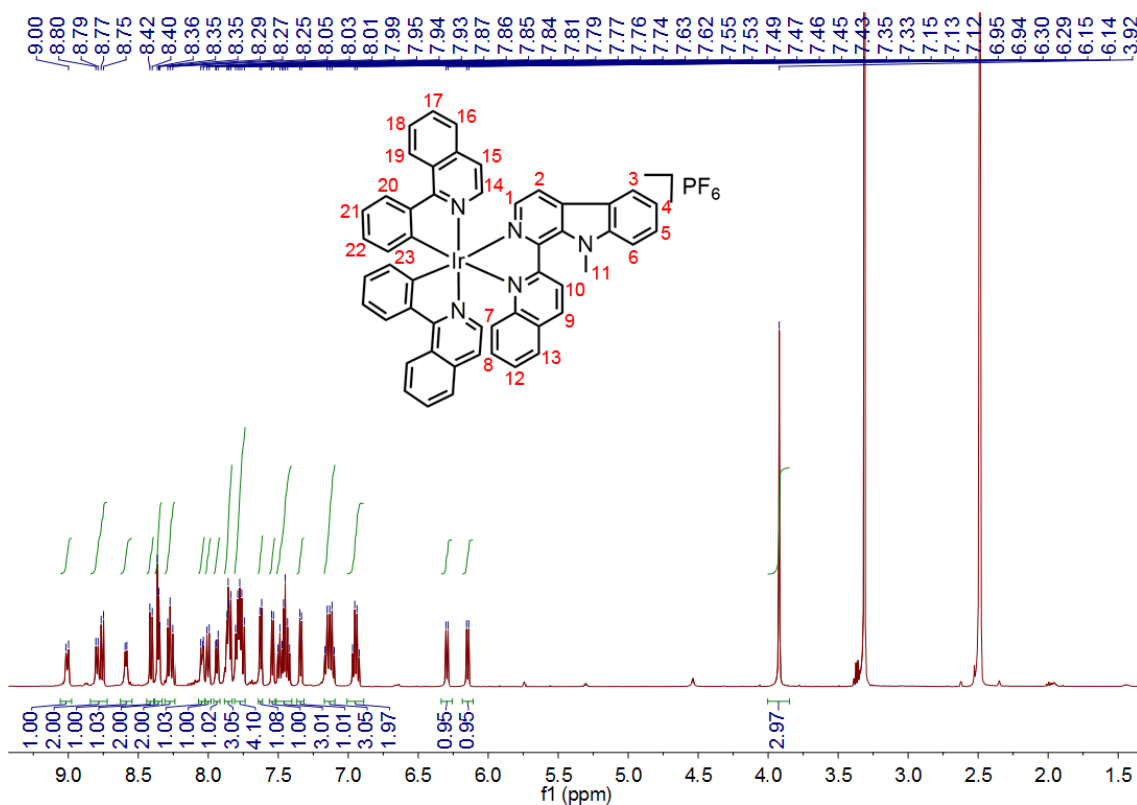
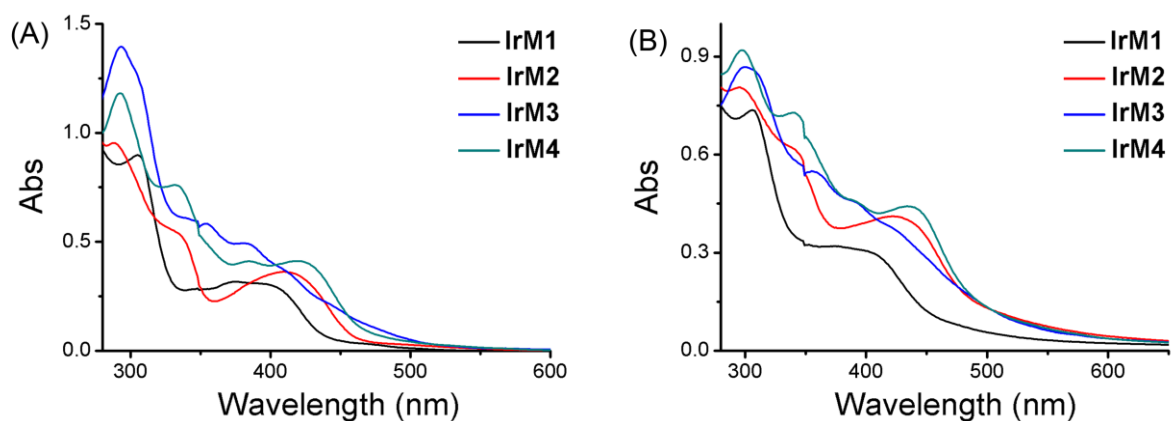
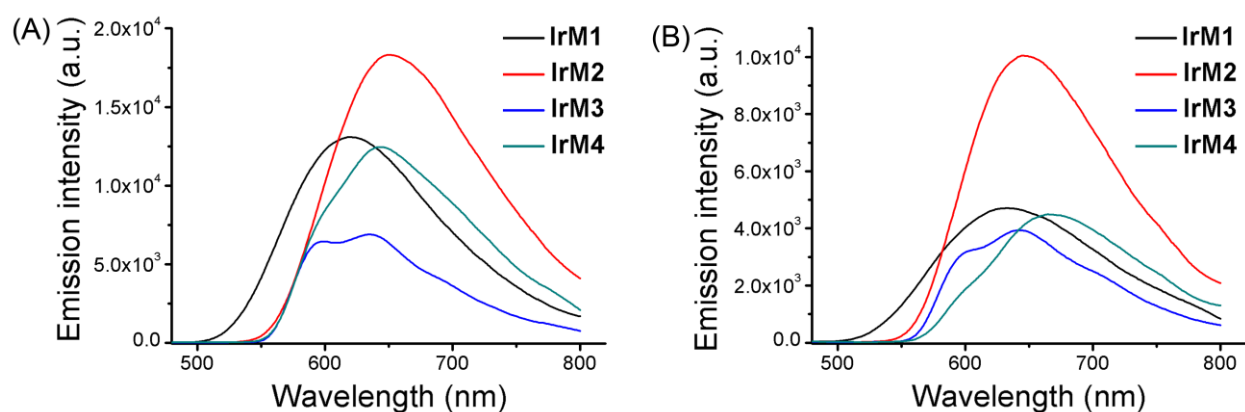


Fig. S6 <sup>1</sup>H NMR spectrum of IrM4 in d<sub>6</sub>-DMSO.



**Fig. S7** UV/Vis spectra of complexes IrM1–IrM4 (10  $\mu\text{M}$ ) measured in (A)  $\text{CH}_3\text{CN}$  and (B) PBS at 25  $^\circ\text{C}$ .



**Fig. S8** Emission spectra of complexes IrM1–IrM4 (10  $\mu\text{M}$ ) measured in (A)  $\text{CH}_3\text{CN}$  and (B) PBS at 25  $^\circ\text{C}$ .  $\lambda_{\text{ex}} = 405 \text{ nm}$ .

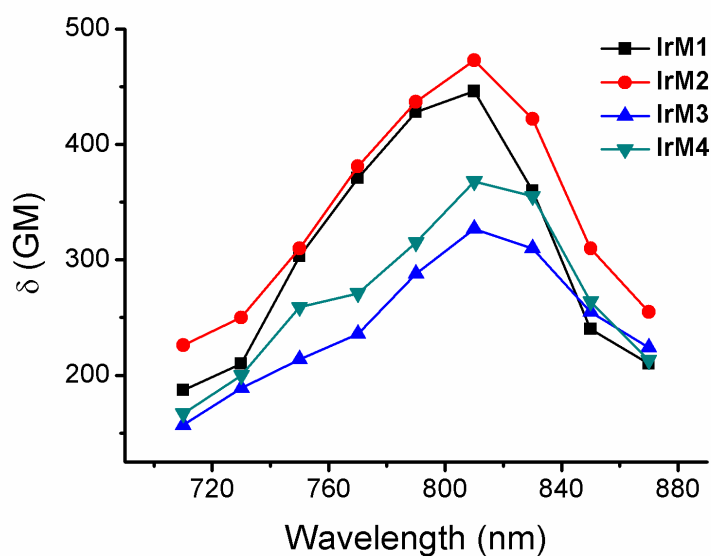


**Fig. S9** Two-photon absorption cross-sections ( $\delta$ ) of complexes **IrM1–IrM4** at excitation wavelengths between 710 and 870 nm.

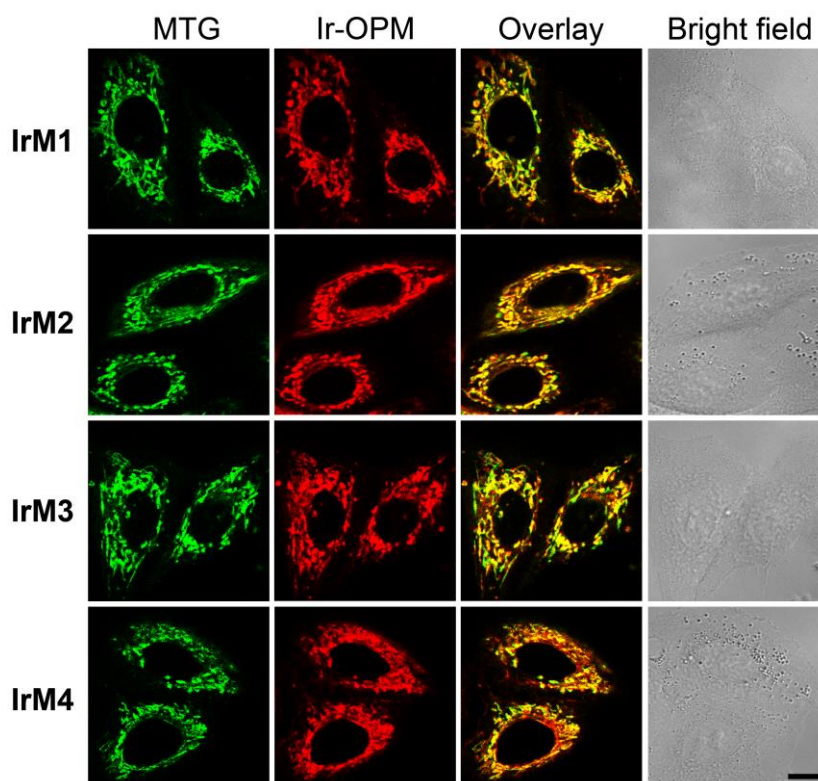


**Fig. S10** CLSM images of A549 cells co-labeled with **IrM1** (1  $\mu$ M, 10 min), **IrM2** (1  $\mu$ M, 10 min), **IrM3** (4  $\mu$ M, 10 min), **IrM4** (4  $\mu$ M, 10 min) and MitoTracker Green (MTG; 150 nM, 30 min).  $\lambda_{\text{ex}}$  = 488 nm (MTG) and 405 nm (Ir-OPM);  $\lambda_{\text{em}}$  = 500–530 nm (MTG) and 600–680 nm (**IrM1–IrM4**). All images share the same scale bar, 10  $\mu$ m.

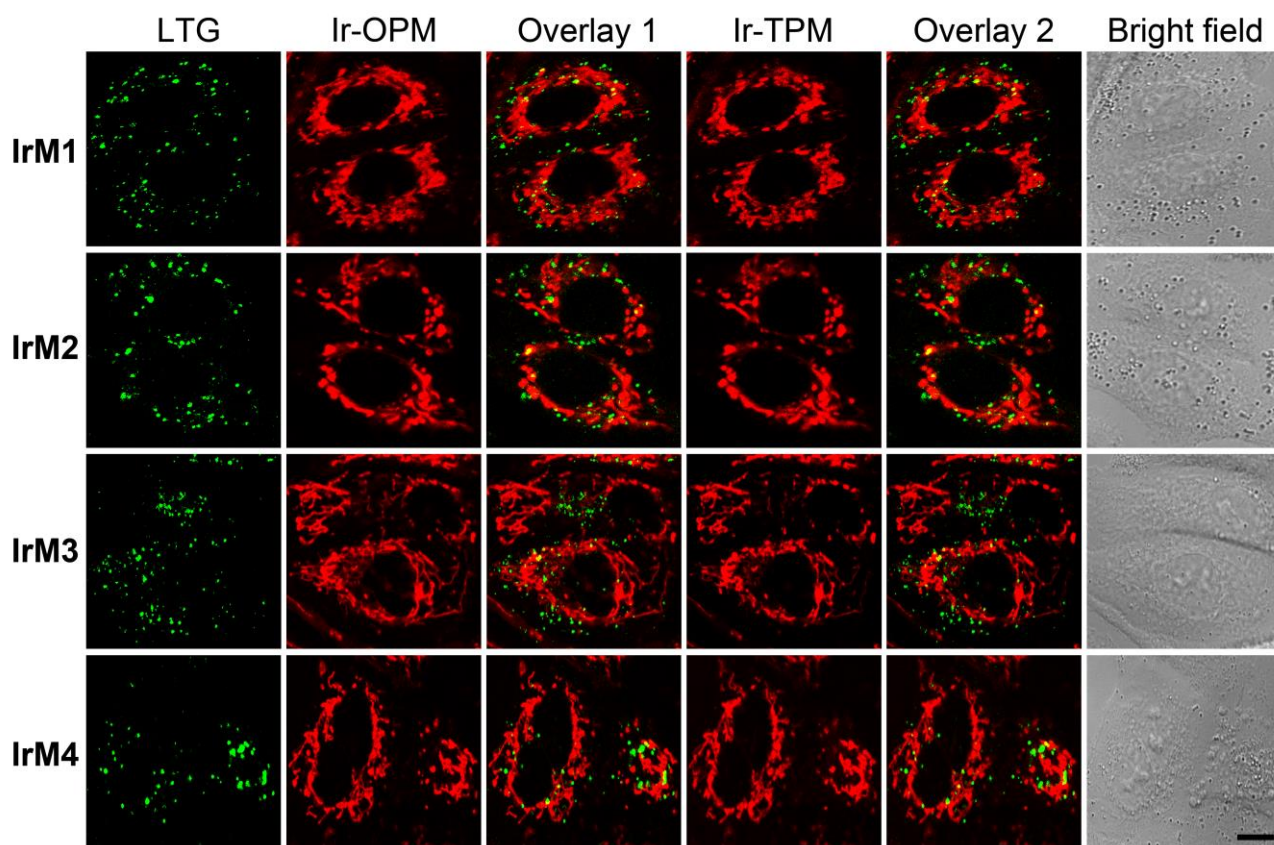


**Fig. S11** CLSM images of A549 cells co-labeled with **IrM1** (1  $\mu$ M, 10 min), **IrM2** (1  $\mu$ M, 10 min), **IrM1** (4  $\mu$ M, 10 min), **IrM4** (4  $\mu$ M, 10 min) and LysoTracker Green DND-26 (LTG; 150 nM, 30 min).  $\lambda_{\text{ex}} = 488$  nm for LTG;  $\lambda_{\text{ex}} = 405$  nm for Ir-OPM;  $\lambda_{\text{ex}} = 810$  nm for Ir-TPM;  $\lambda_{\text{em}} = 500\text{--}530$  nm for LTG;  $\lambda_{\text{em}} = 600\text{--}680$  nm for **IrM1**–**IrM4**. Overlay 1: Overlay of the LTG and Ir-OPM columns. Overlay 2: Overlay of the LTG and Ir-TPM columns. All images share the same scale bar, 10  $\mu$ m.

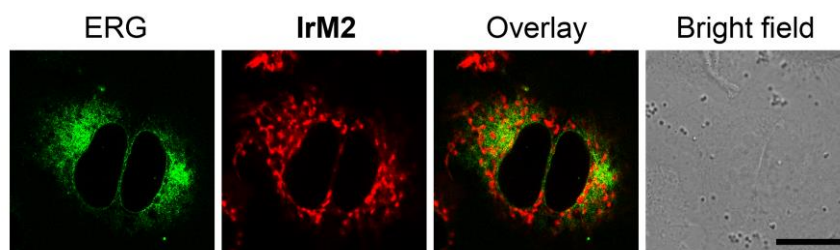


**Fig. S12** CLSM images of A549 cells co-labeled with **IrM2** (1  $\mu$ M, 10 min) and ER-Tracker Green (ERG; 5  $\mu$ M, 30 min).  $\lambda_{\text{ex}} = 488$  nm for ERG;  $\lambda_{\text{ex}} = 810$  nm for **IrM2**;  $\lambda_{\text{em}} = 500\text{--}520$  nm for ERG;  $\lambda_{\text{em}} = 600\text{--}680$  nm for **IrM2**. All images share the same scale bar, 10  $\mu$ m.

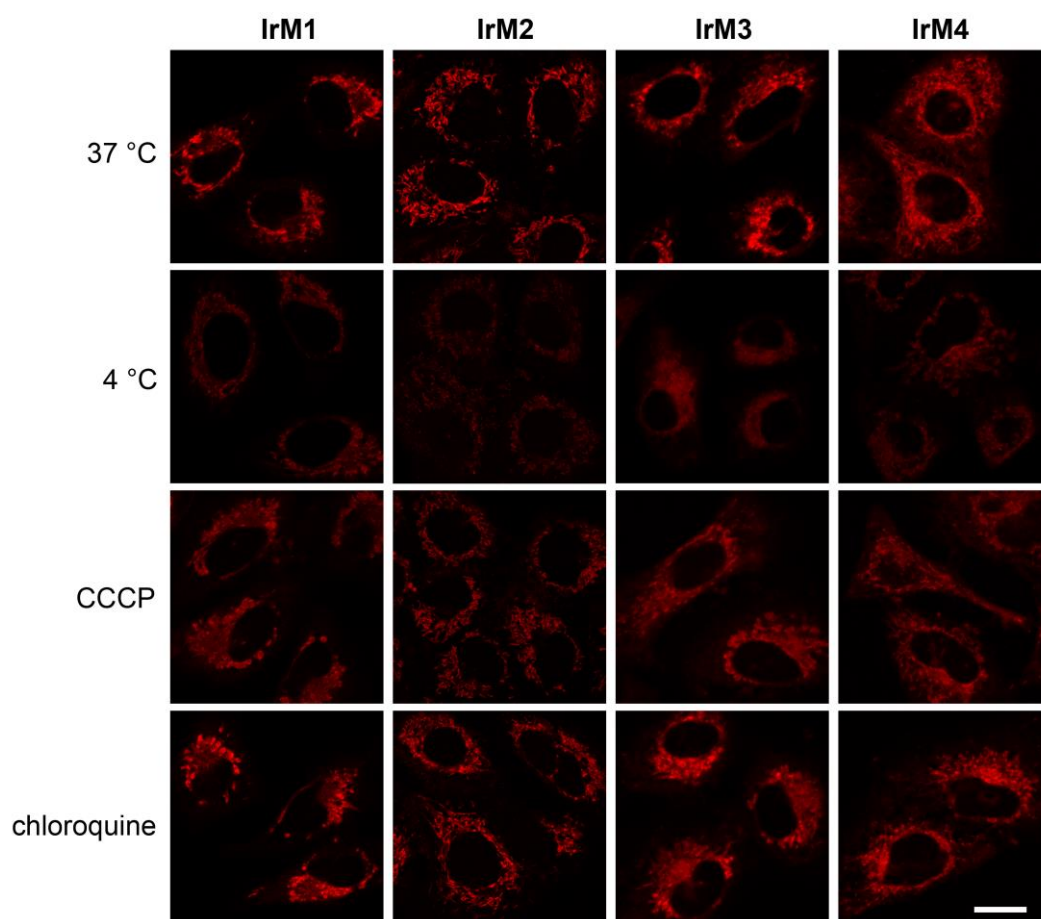


**Fig. S13** Cellular uptake mechanisms of **IrM1–IrM4**. A549 cells were incubated with **IrM1–IrM4** (2  $\mu$ M, 10 min) under different temperature, pretreated with CCCP (20  $\mu$ M, 1 h) or chloroquine (50  $\mu$ M, 1 h).  $\lambda_{\text{ex}} = 405 \text{ nm}$ ;  $\lambda_{\text{em}} = 600\text{--}680 \text{ nm}$ . Scale bar: 20  $\mu$ m.



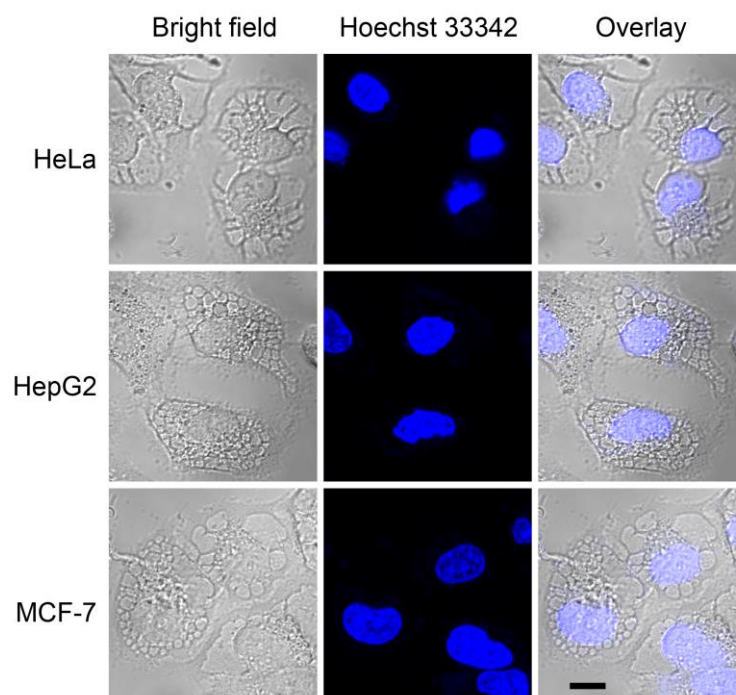


**Fig. S14** Representative images of Hoechst 33342 stained HeLa, HepG2 and MCF-7 cells after treatment with 4  $\mu$ M complex **IrM2** for 24 h. Scale bar: 10  $\mu$ m.

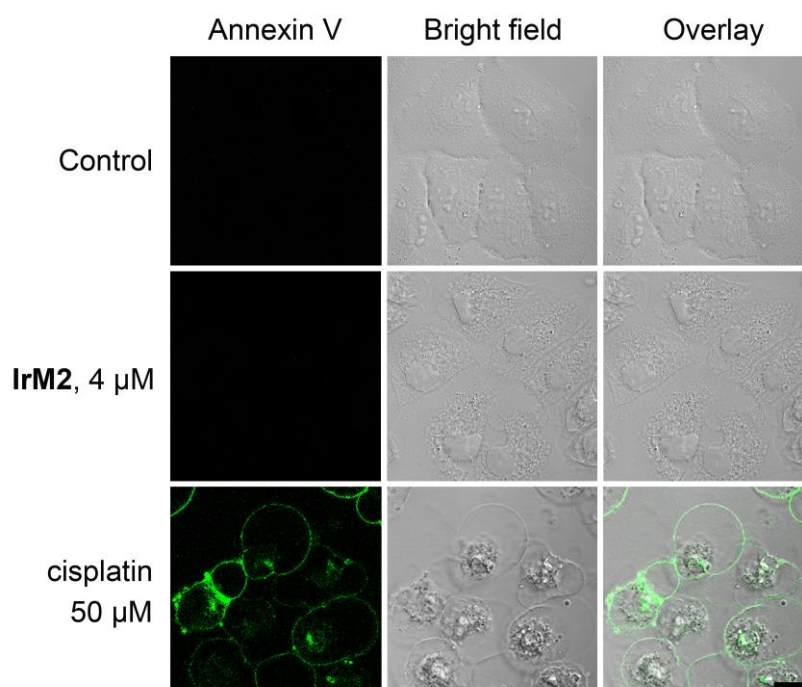


**Fig. S15** Representative confocal images of annexin V labeled A549 cells after treatment with 4  $\mu$ M complex **IrM2** or 50  $\mu$ M cisplatin for 24 h. Scale bar: 10  $\mu$ m.

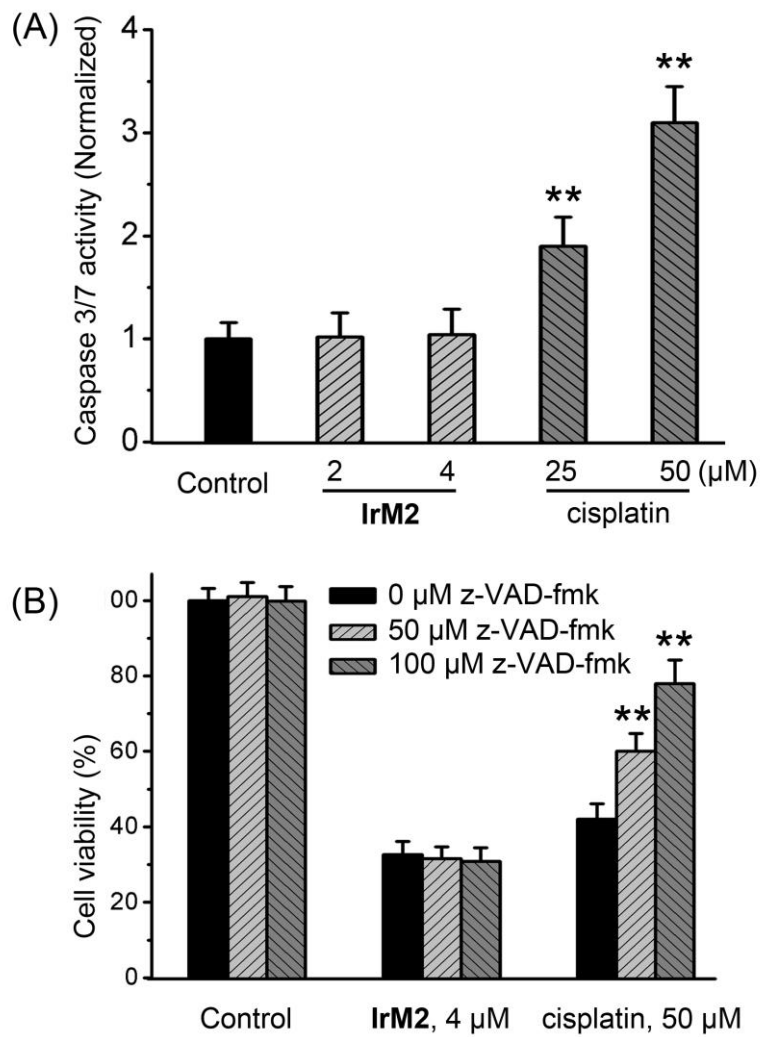


**Fig. S16** (A) Detection of caspase-3/7 activity after A549 cells were treated with **IrM2** or cisplatin at the indicated concentrations for 6 h. (B) A549 cells were treated with **IrM2** (4 μM) or cisplatin (50 μM) for 24 h with or without pretreatment of z-VAD-fmk (50 or 100 μM) for 1 h. Cell viability was measured by MTT assay. Data are represented as means ± SD of three independent experiments. \*\*p < 0.01, as compared with the control groups.

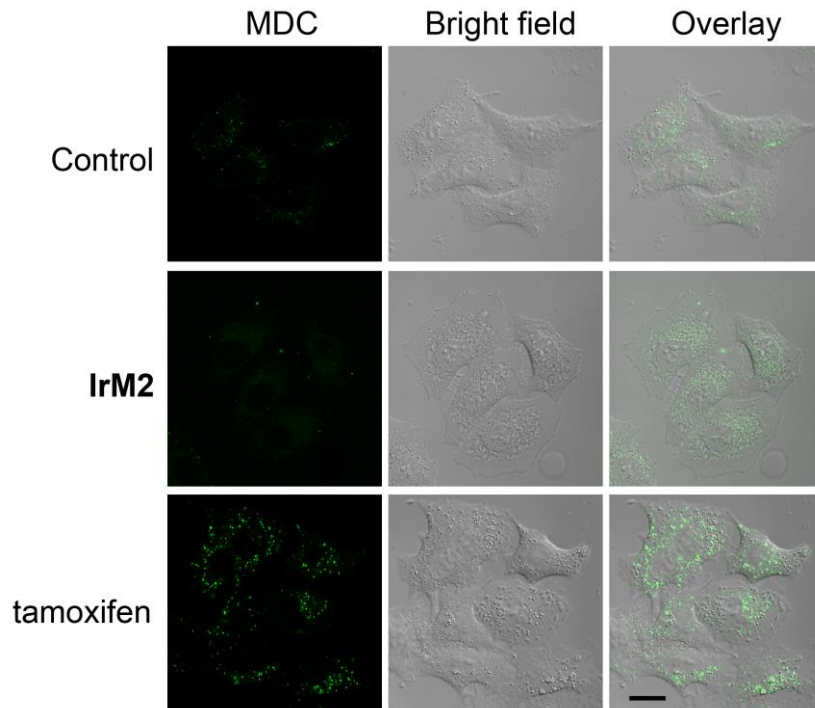


**Fig. S17** Representative confocal images of MDC stained A549 cells after treatment with 4  $\mu\text{M}$  complex **IrM2** or 10  $\mu\text{M}$  tamoxifen for 12 h. Scale bar: 10  $\mu\text{m}$ .



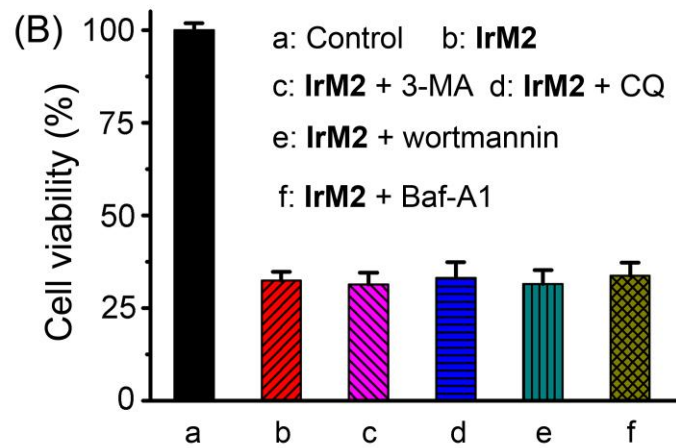
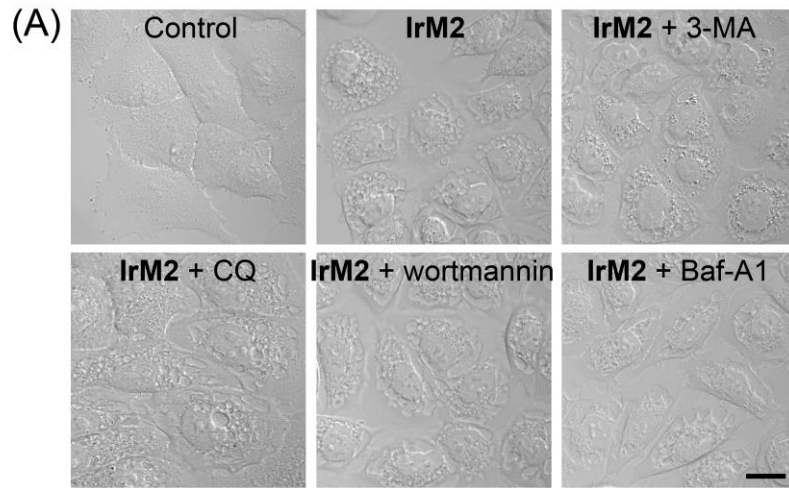


**Fig. S18** (A) Bright field confocal images and (B) cell viability (24 h) of complex **IrM2** (4  $\mu$ M) treated A549 cells in the absence and presence of various autophagy inhibitors. 3-MA: 1 mM; CQ: 50  $\mu$ M; wortmannin: 100 nM; Baf-A1: 20 nM.

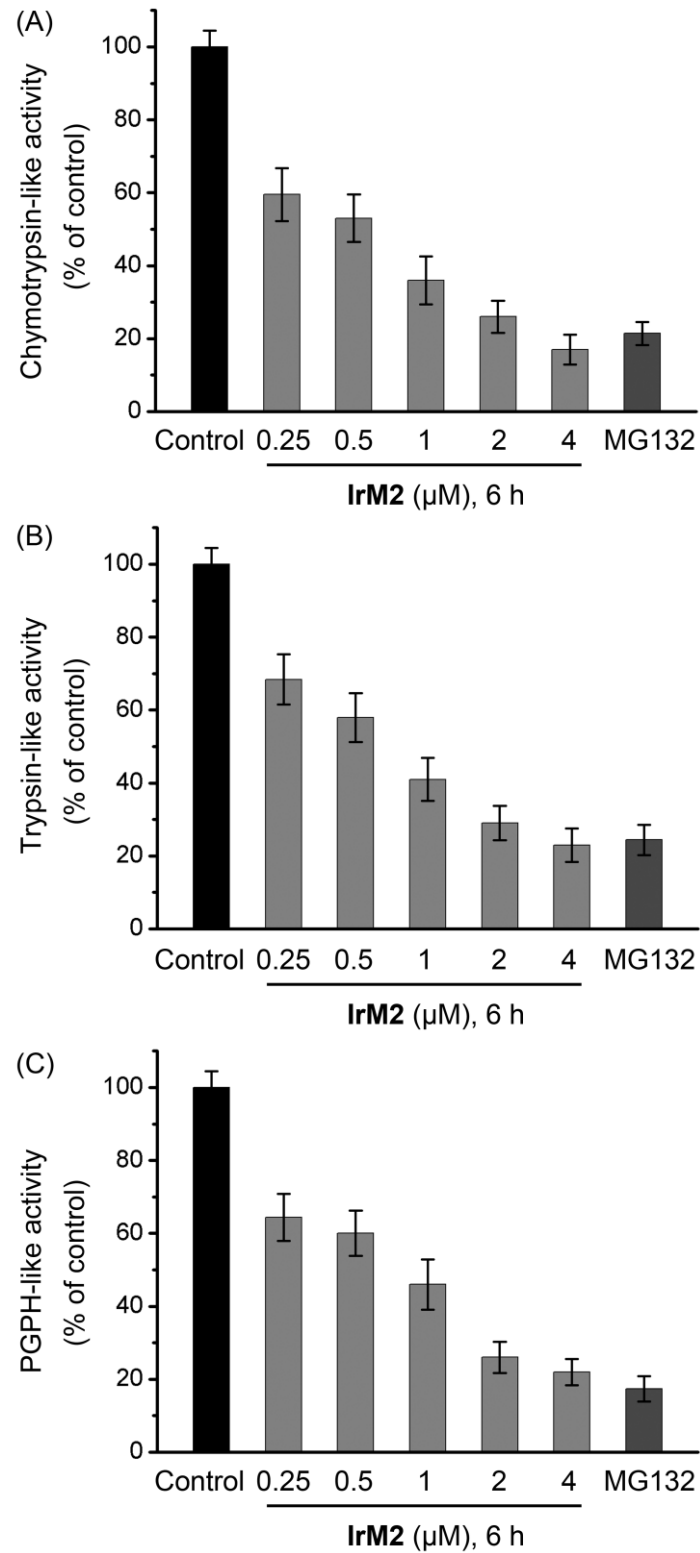


**Fig. S19** Cellular proteasomal activity in A549 cells treated with indicated concentrations of IrM2 or 5 μM MG132 for 6 h.

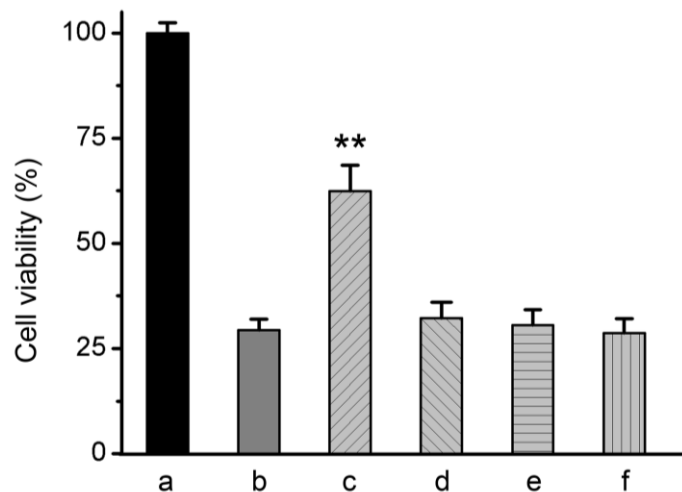


**Fig. S20** Cell viability (24 h) of **IrM2** (4  $\mu$ M) treated A549 cells in the absence and presence of various inhibitors. a, control; b, **IrM2**; c, **IrM2**+U0126 (20  $\mu$ M); d, **IrM2**+CHX (2 mM); e, **IrM2**+4-PBA (5 mM); f, **IrM2**+necrostatin-1 (100  $\mu$ M). \*\* $p < 0.01$ , as compared with **IrM2**-treated group (b).

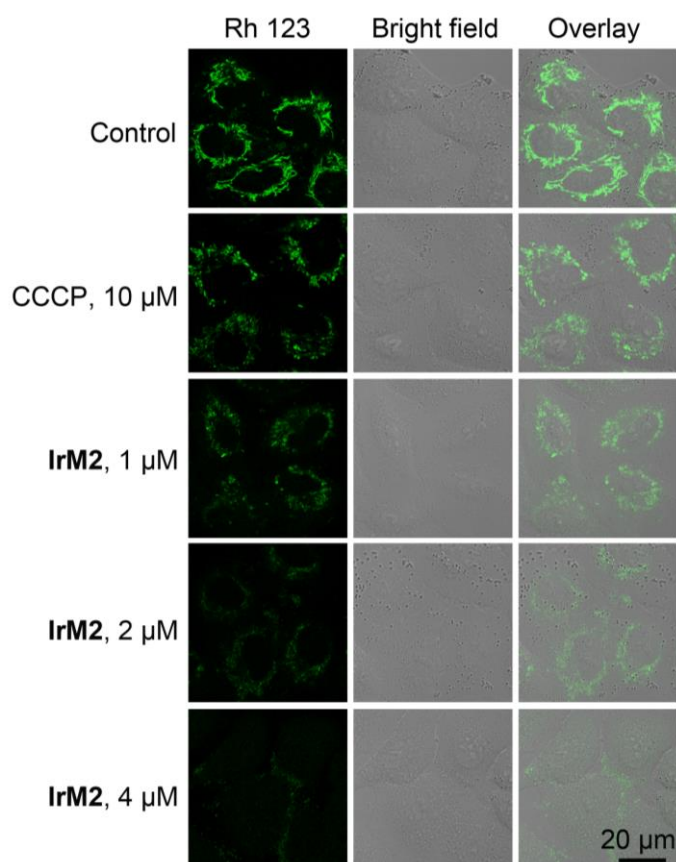


**Fig. S21** Effects of **IrM2** on MMP analyzed by confocal microscopy. A549 cells were treated with indicated concentrations of **IrM2** for 1 h and then stained with Rhodamine 123.

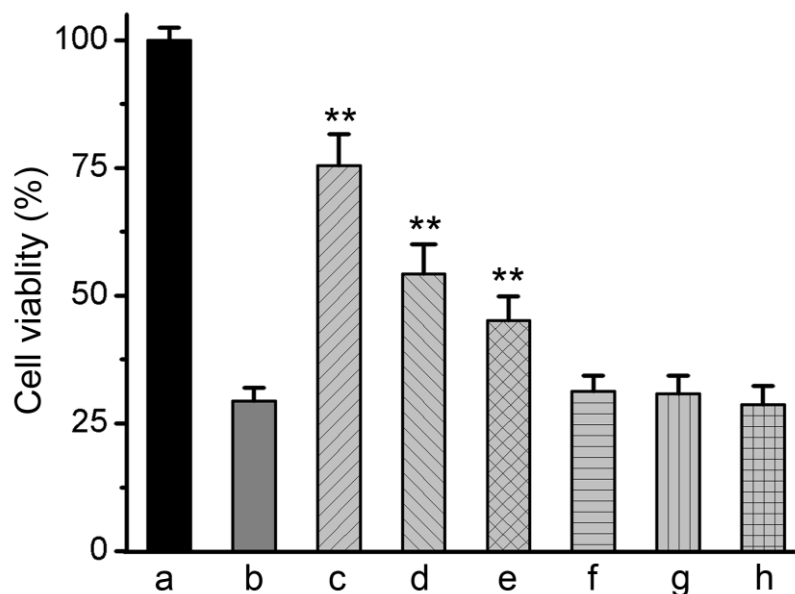


**Fig. S22** Cell viability (24 h) of IrM2 (4 μM) treated A549 cells in the absence and presence of various ROS inhibitors. a, control; b, IrM2; c, IrM2+MnTBAP (100 μM); d, IrM2+catalase (1000 U/ml); e, IrM2+NAC (10 mM); f, IrM2+mannitol (10 mM); g, IrM2+KI (10 mM); h, IrM2+NaN<sub>3</sub> (10 mM). \*\* $p < 0.01$ , as compared with IrM2-treated group (b).

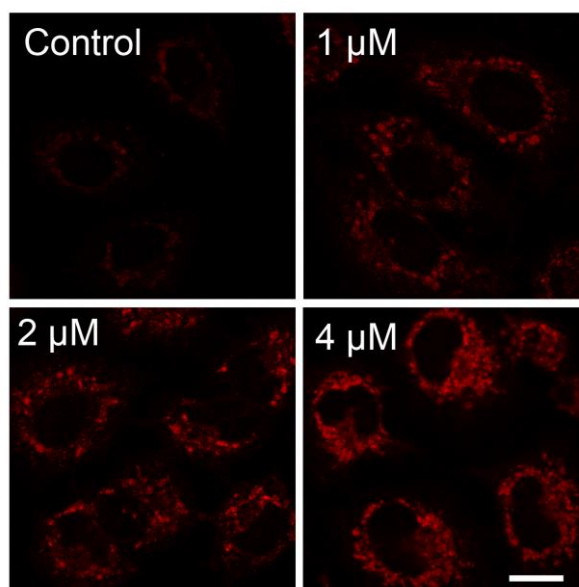


**Fig. S23** Fluorescence images of A549 cells incubated with (A) control, (B) 1 μM, (C) 2 μM and (D) 4 μM IrM2 for 1 h, followed by staining with MitoSOX-Red (5 μM) for 10 min.  $\lambda_{ex} = 514$  nm;  $\lambda_{em} = 570-600$  nm. scale bar: 20 μm.

**Table S1** Crystallographic data of **IrM2**, **IrM3•CH<sub>2</sub>Cl<sub>2</sub>** and **IrM4•CH<sub>2</sub>Cl<sub>2</sub>**

Complex	<b>IrM2</b>	<b>IrM3•CH<sub>2</sub>Cl<sub>2</sub></b>	<b>IrM4•CH<sub>2</sub>Cl<sub>2</sub></b>
CCDC no.	1812906	1814616	1812909
Empirical formula	C <sub>43</sub> H <sub>31</sub> N <sub>5</sub> F <sub>6</sub> PIr	C <sub>47</sub> H <sub>33</sub> N <sub>5</sub> F <sub>6</sub> PIr•CH <sub>2</sub> Cl <sub>2</sub>	C <sub>51</sub> H <sub>35</sub> N <sub>5</sub> F <sub>6</sub> PIr•CH <sub>2</sub> Cl <sub>2</sub>
Molecular weight	954.90	1089.88	1137.92
Description	Block, red	Block, red	Block, red
Temperature (K)	293 K	293 K	298 K
λ (Å)	1.54184	0.71073	0.71073
Crystal system	monoclinic	monoclinic	monoclinic
Space group	P2 <sub>1</sub> /n	P2 <sub>1</sub> /c	P2 <sub>1</sub> /c
a (Å)	12.6047(3)	14.5049(8)	13.7563(10)
b (Å)	14.1338(4)	12.0032(6)	26.9979(14)
c (Å)	20.6321(6)	25.2576(16)	12.3453(8)
α (°)	90	90	90
β (°)	98.500(2)	94.719(2)	92.268(2)
γ (°)	90	90	90
Volume, Å <sup>3</sup>	3635.28(17)	4382.6(4)	4581.3(5)
Z	4	4	4
μ/mm <sup>-1</sup>	8.145	3.272	3.134
F(000)	1880.0	2152.0	2248.0
θ <sub>max</sub> (deg)	74.065	27.480	27.480
Completeness	to 0.984	0.940	0.998
ρ <sub>calc</sub> (g/cm <sup>3</sup> )	1.745	1.652	1.650
[R <sub>int</sub> ]	0.0451	0.0694	0.0575
R1 <sup>a</sup> [I > 2σ(I)]	0.0326	0.0535	0.0593
wR2 <sup>a</sup>	0.0849	0.1759	0.1894
GOF <sup>b</sup>	1.036	1.062	0.987

$${}^a R1 = \sum |F_o| - |F_c| / \sum |F_o|, wR2 = \left\{ \frac{\sum [w(F_o^2 - F_c^2)^2]}{\sum [w(F_o^2)]} \right\}^{1/2} {}^b GOF = \left\{ \frac{\sum [w(F_o^2 - F_c^2)^2]}{(n-p)} \right\}^{1/2}$$

where *n* is the number of data and *p* is the number of parameters refined.

**Table S2** Selected bond lengths (Å) and bond angles (deg) of **IrM2** and **IrM4**·CH<sub>2</sub>Cl<sub>2</sub>

Complex	<b>IrM2</b>		<b>IrM3</b> ·CH <sub>2</sub> Cl <sub>2</sub>		<b>IrM4</b> ·CH <sub>2</sub> Cl <sub>2</sub>	
bond lengths (Å)	Ir1–N1	2.042(3)	Ir1–N1	2.042(6)	Ir1–N1	2.043(5)
	Ir1–N2	2.059(3)	Ir1–N2	2.050(6)	Ir1–N2	2.033(6)
	Ir1–N3	2.213(3)	Ir1–N3	2.154(6)	Ir1–N3	2.242(6)
	Ir1–N4	2.132(3)	Ir1–N4	2.162(5)	Ir1–N4	2.146(6)
	Ir1–C15	2.010(4)	Ir1–C15	2.032(7)	Ir1–C15	2.010(6)
	Ir1–C30	2.028(4)	Ir1–C30	2.002(8)	Ir1–C30	2.002(7)
bond angles (deg)	N1–Ir1–N3	96.95(13)	N1–Ir1–N3	86.4(2)	N1–Ir1–N3	99.8(2)
	N3–Ir1–N4	76.01(13)	N3–Ir1–N4	76.7(2)	N3–Ir1–N4	76.1(2)
	N1–Ir1–C15	80.25(16)	N1–Ir1–C15	78.7(3)	N1–Ir1–C15	79.9(2)
	C15–Ir1–N4	96.36(14)	C15–Ir1–N4	176.4(3)	C15–Ir1–N4	96.9(2)
	N1–Ir1–N2	173.76(13)	N1–Ir1–N2	96.7(2)	N1–Ir1–N2	175.9(2)
	C30–Ir1–C15	82.45(16)	C30–Ir1–C15	90.0(3)	C30–Ir1–C15	85.4(3)

**Table S3** Photophysical data of complexes **IrM1–IrM4**

Complex	Medium	$\lambda_{em}^a$ /nm	$\Phi^b$	$\tau^c$ /ns
<b>IrM1</b>	CH <sub>2</sub> Cl <sub>2</sub>	611	0.52	319
	CH <sub>3</sub> CN	619	0.16	124
	PBS	632	0.027	368
<b>IrM2</b>	CH <sub>2</sub> Cl <sub>2</sub>	646	0.54	378
	CH <sub>3</sub> CN	650	0.17	192
	PBS	645	0.038	469
<b>IrM3</b>	CH <sub>2</sub> Cl <sub>2</sub>	594, 633	0.19	544
	CH <sub>3</sub> CN	598, 634	0.058	216
	PBS	599, 641	0.016	552
<b>IrM4</b>	CH <sub>2</sub> Cl <sub>2</sub>	645	0.41	347
	CH <sub>3</sub> CN	643	0.10	196
	PBS	665	0.018	369

<sup>a</sup> Emission maximum,  $\lambda_{ex} = 405$  nm. <sup>b</sup> The emission quantum yields were determined using [Ru(bpy)<sub>3</sub>]Cl<sub>2</sub> in N<sub>2</sub>-saturated CH<sub>2</sub>Cl<sub>2</sub> ( $\Phi = 0.059$ ),<sup>9</sup> CH<sub>3</sub>CN ( $\Phi = 0.062$ )<sup>10</sup> and PBS ( $\Phi = 0.042$ )<sup>11</sup> as the references. <sup>c</sup> The lifetimes were measured at the emission maxima.

**Table S4.** Lipophilicity and cellular uptake of complexes **IrM1–IrM4**

Complex	Lipophilicity (log $P_{o/w}$ ) <sup>a</sup>	Amount of iridium (ng per 10 <sup>6</sup> cells) <sup>b</sup>		
		Whole cell	Mitochondria	Percentage in mitochondria
<b>IrM1</b>	1.42	750	548	73%
<b>IrM2</b>	1.56	823	626	76%
<b>IrM3</b>	1.52	529	360	68%
<b>IrM4</b>	1.77	369	244	66%

<sup>a</sup> Log  $P_{o/w}$  is defined as the logarithmic ratio of Ir(III) concentration in *n*-octanol to that in the aqueous phase. <sup>b</sup> Amount of iridium in A549 cells and the mitochondrial fractions was determined by ICP-MS after cells were treated with Ir(III) complexes (10  $\mu$ M) at 37 °C for 2 h.

## Supporting references

1. L. He, S. Y. Liao, C. P. Tan, R. R. Ye, Y. W. Xu, M. Zhao, L. N. Ji and Z. W. Mao, *Chem.-Eur. J.*, 2013, **19**, 12152–12160.
2. C. Y. Li, M. X. Yu, Y. Sun, Y. Q. Wu, C. H. Huang and F. Y. Li, *J. Am. Chem. Soc.*, 2011, **133**, 11231–11239.
3. L. He, Y. Li, C. P. Tan, R. R. Ye, M. H. Chen, J. J. Cao, L. N. Ji and Z. W. Mao, *Chem. Sci.*, 2015, **6**, 5409–5418.
4. G. M. Sheldrick, *Acta Crystallogr. A*, 2008, **64**, 112–122.
5. N. S. Makarov, M. Drobizhev and A. Rebane, *Opt. Express*, 2008, **16**, 4029-4047.
6. C. Xu and W. W. Webb, *J. Opt. Soc. Am. B*, 1996, **13**, 481–491.
7. L. He, C. P. Tan, R. R. Ye, Y. Z. Zhao, Y. H. Liu, Q. Zhao, L. N. Ji and Z. W. Mao, *Angew. Chem., Int. Ed.*, 2014, **53**, 12137–12141.
8. J. J. Cao, C. P. Tan, M. H. Chen, N. Wu, D. Y. Yao, X. G. Liu, L. N. Ji and Z. W. Mao, *Chem. Sci.*, 2017, **8**, 631–640.
9. D. Pucci, A. Bellusci, A. Crispini, M. Ghedini, N. Godbert, E.I. Szerb and A. M. Talarico, *J. Mater. Chem.*, 2009, **19**, 7643–7649.
10. D. S. Tyson and F. N. Castellano, *J. Phys. Chem. A*, 1999, **103**, 10955–10960.
11. J. Van Houten and R. J. Watts, *J. Am. Chem. Soc.*, 1976, **98**, 4853–4858.